Radiología 63 (2021) 270–290

RADIOLOGÍA

www.elsevier.es/rx

SERIE: ULTRASOUND OF THE GASTROINTESTINAL TRACT

# Ultrasonography in infectious and neoplastic diseases of the bowel and peritoneum☆

**M.Á. Corral de la Calle**[a,*], **J. Encinas de la Iglesia**[b]

[a] *Servicio de Radiodiagnóstico, Complejo Asistencial de Ávila, Ávila, Spain*
[b] *Servicio de Radiodiagnóstico, Complejo Asistencial de Salamanca, Salamanca, Spain*

Received 16 July 2020; accepted 28 December 2020

**KEYWORDS**
Ultrasonography;
Interventional ultrasonography;
Gastroenteritis;
Enterocolitis;
Peritonitis;
Gastrointestinal tumors;
GIST;
Gastrointestinal tract cancer;
Neuroendocrine tumors;
Peritoneal tumors

**Abstract** Ultrasonography is not the most cited imaging technique for the evaluation of infectious and neoplastic diseases of the gastrointestinal tract and the peritoneum, but it is often the initial technique used in the initial workup for nonspecific clinical syndromes. Despite its limitations, ultrasonography's strengths enable it to provide meaningful diagnostic information.

To discuss the most important ultrasonographic, clinical, and epidemiological findings for infectious disease, we follow a topographical approach: stomach (Anisakis), proximal small bowel (Giardia lamblia, Strongyloides stercoralis, Mycobacterium avium-intracellulare complex, and Cryptosporidium), distal small bowel (Yersinia, Salmonella, and Campylobacter), terminal ileum and cecum (tuberculosis), right colon (Entamoeba histolytica), left colon (Shigella), sigmoid colon and rectum, pancolitis (Clostridium difficile, Cytomegalovirus, and Escherichia coli), and peritoneum.

To discuss the ultrasonographic and clinical findings of the most common neoplastic diseases, we follow a nosological approach: polyploid lesions as precursors of tumors, carcinomas, neuroendocrine tumors, hematological tumors, mesenchymal tumors, and metastases. We briefly discuss tumors of the peritoneum and the use of ultrasonography to guide percutaneous biopsy procedures.


**PALABRAS CLAVE**
Ecografía;
Ecografía intervencionista;
Gastroenteritis;

**Ecografía de la patología infecciosa y tumoral del intestino y el peritoneo**

**Resumen** La ecografía no es la técnica de imagen más citada para la valoración de la patología infecciosa y tumoral del tubo digestivo y el peritoneo, pero a menudo es la inicialmente empleada ante cuadros inespecíficos. Aunque no exenta de limitaciones, presenta fortalezas

☆ Please cite this article as: Corral de la Calle MÁ, Encinas de la Iglesia J, Ecografía de la patología infecciosa y tumoral del intestino y el peritoneo. Radiología. 2021;63:270–290.

* Corresponding author.
*E-mail address:* migcorral@gmail.com (M.Á. Corral de la Calle).

Enterocolitis;
Peritonitis;
Tumores gastrointestinales;
Tumores del estroma gastrointestinal;
Cáncer del tracto gastrointestinal;
Tumores neuroendocrinos;
Tumores peritoneales

que pueden permitirle aportar información diagnóstica significativa. Discutimos los datos ecográficos, clínicos y epidemiológicos más relevantes en la patología infecciosa, siguiendo un abordaje topográfico: estómago (*Anisakis*), intestino delgado proximal (*Giardia lamblia*, *Strongyloides stercolaris*, Complejo *Mycobacterium-avium-intracelulare* y *Criptosporidium*), intestino delgado distal (*Yersinia*, *Salmonella*, *Campylobacter*) íleon terminal y ciego (tuberculosis), colon derecho (*Entamoeba histolytica*), colon izquierdo (*Shigella*), recto-sigma, pancolitis (*Clostridium difficile*, Citomegalovirus, *Escherichia coli*) y peritoneo. Abordamos los hallazgos ecográficos y clínicos de la patología neoplásica más frecuente con un patrón nosológico: lesiones polipoideas como precursoras de neoplasias, carcinomas, tumores neuroendocrinos, hematológicos, mesenquimales y metástasis. Discutimos brevemente la patología tumoral del peritoneo y la ecografía como guía de biopsia percutánea.


## Infectious diseases of the bowel and peritoneum

Many different pathogens can cause bowel infections. The most common are viruses, but they also include bacteria, fungi and parasites. Common symptoms are abdominal pain, nausea and vomiting, diarrhoea (possibly watery and copious or with blood) and fever. They very often have a self-limited course, with few clinical repercussions, and the diagnosis tends to be based on epidemiological data, stool cultures or serology. Imaging tests are not usually required, but sometimes they do play an important role.

Although the usual imaging technique in this setting is computed tomography (CT), ultrasound can be very useful. Ultrasound is often the first test requested in patients with nonspecific abdominal pain. In particular, it should be used in children and pregnant women. In the monitoring of severe cases, ultrasound can help assess the severity and extent of bowel involvement and rule out surgical complications, with the advantage of its greater availability, portability, and lack of radiation and nephrotoxic contrast. It also gives us additional information by providing the most dynamic assessment of bowel peristalsis.

The typical ultrasound appearance of bowel infection is thickening of the wall, generally keeping the normal layer structure, with the mucosa and submucosa affected, but not involving the muscle layer. There may be accompanying local or regional lymphadenopathy, inflammatory changes in the adjacent fatty planes or free fluid. In cases of secretory diarrhoea, the initial finding is fluid-filled bowel loops. Unlike in neoplastic lesions, with infection, Doppler shows increased vascularisation with low resistance indices (<0.60).[1] Special techniques such as contrast-enhanced ultrasound and elastography are of little use in this context.[2]

These findings are nonspecific and do not provide a definitive aetiological diagnosis, but some characteristics, such as the distribution of the abnormalities, the patient's immune status and the presence of extraintestinal manifestations help direct us towards the origin of the condition. We have used a topographical approach to present some of the most common causes of gastrointestinal infectious diseases in our setting, a summary of which is shown in Table 1.

## Gastrointestinal tract

### Stomach

#### Anisakis

Anisakiasis occurs after ingestion of the parasite larva in raw or undercooked fish. Although the first cases were described in Asian countries, it has become globalised. When it affects the stomach, as it usually does, the symptoms develop in less than 24 h. It causes severe acute pain in the epigastrium, nausea and vomiting, and can mimic pancreatobiliary disease. Ultrasound, often urgent, shows significant diffuse thickening of the stomach wall (Fig. 1A) and ascites, suggesting a differential diagnosis with cancer (diffuse lymphoma or adenocarcinoma) or eosinophilic gastritis (Fig. 1B).

Much less common, intestinal anisakiasis involves the terminal ileum and can spread to the colon, delaying symptoms for up to five days and mimicking inflammatory bowel disease, appendicitis, diverticulitis or bowel obstruction. It causes segmental thickening of the ileum wall with slight proximal dilation and ascites.

Patients can have both at the same time. They will occasionally have allergic symptoms, and eosinophilia is common. Diagnosis is guided by the epidemiological history and confirmed by endoscopic detection of the larva, eosinophilic infiltration of the wall in histological study, and the increase in specific IgE.[3–5]

### Proximal small bowel

#### Giardia lamblia

Parasitic disease which affects the duodenum and jejunum, causing, diarrhoea and malabsorption. People with hypogammaglobulinaemia are particularly prone. It is common in developing countries with poor hygiene conditions, in children and in international travellers. Findings include a fluid-filled bowel lumen with increased peristalsis and normal wall thickness,[6] or oedema of the submucosa, occasionally with a pseudo-nodular appearance due to lymphoid hyperplasia, in the context of an autoimmune disorder.[7] It is frequently accompanied by mesenteric lymphadenopathy,

**Table 1** Summary of gastrointestinal tract infections.

| Location | Cause | Immune status | Transmission | Typical findings | Differential diagnosis |
|---|---|---|---|---|---|
| Stomach | *Anisakis* | Immunocompetent | Parasite larva in raw or undercooked fish | Marked thickening of the stomach wall and ascites. Peripheral blood eosinophilia | Lymphoproliferative syndrome<br>Gastric adenocarcinoma<br>Eosinophilic gastritis |
| Proximal small bowel | *Giardia* | Hypogammaglobulinaemia | Poor hygiene conditions and international travellers | Increased peristalsis, fluid-filled lumen and lymphadenopathy | Lymphoproliferative syndrome<br>Eosinophilic enteritis Whipple's disease |
| | *Mycobacterium avium intracellulare* | Immunosuppressed (CD4 < 100/mL) | | Voluminous mesenteric and retroperitoneal lymphadenopathy. Visceral lesions (liver, spleen) | Lymphoproliferative syndrome Whipple's disease |
| | *Cryptosporidium* | Immunosuppressed (CD4 < 50/mL) | | No lymphadenopathy. Cholangiopathy | Cytomegalovirus |
| Distal small bowel (distal ileum) | *Yersinia* | Immunocompetent | Pork. Developed countries | Young patients. Enlarged lymph nodes and normal appendix. Accompanying pharyngitis | Appendicitis<br>Crohn's disease |
| | *Salmonella* | Immunocompetent (children) | Eggs, poultry meat. Developed countries | Acalculous cholecystitis. Splenomegaly | Appendicitis<br>Crohn's disease |
| | *Campylobacter* | Immunocompetent | Poultry meat. Developed countries | Extraintestinal involvement (cholecystitis, peritonitis, arthritis, myocarditis). Guillain-Barré syndrome | Appendicitis<br>Crohn's disease |
| Distal ileum and caecum | Tuberculosis | Immunosuppressed, although with CD < 200/mL | Contaminated milk or pulmonary tuberculosis | Thickening of the ileocaecal valve and the medial wall of the caecum. Enlarged lymph nodes (calcified). Peritoneal involvement | Crohn's disease<br>Lymphoproliferative syndrome<br>Peritoneal carcinomatosis |
| Right colon | *Entamoeba* | Immunocompetent | Tropical regions. Travellers | Spares the ileum. Liver abscess | Lymphoproliferative syndrome<br>Neoplasm |
| Left colon | *Shigella* | Immunocompetent | Faecal-oral in less developed countries | Dysentery. Haemolytic uraemic syndrome (children) and reactive arthritis (adults) | Other causes of dysentery (*E. coli*, *Clostridium*, etc) |
| Rectum and sigmoid colon | Herpesvirus, gonorrhoea and chlamydia | Immunocompetent | Sexual transmission | Rectal bleeding and purulent discharge (also urethral). Lymph node abscesses (*Chlamydia*) and vesicles in mucosa (herpes) | Inflammatory bowel disease |
| Pancolitis | *Clostridium difficile* | Immunocompetent | Broad-spectrum antibiotics | Very marked thickening of the submucosa with little pericolonic involvement (disproportion) | Inflammatory bowel disease<br>Ischaemic colitis |
| | Cytomegalovirus | Immunosuppressed | | No lymphadenopathy. Cholangiopathy | Inflammatory bowel disease |
| | *Escherichia coli* | Immunocompetent | Bad meat | Traveller's diarrhoea (mild) or dysentery (severe) | Other causes of dysentery |

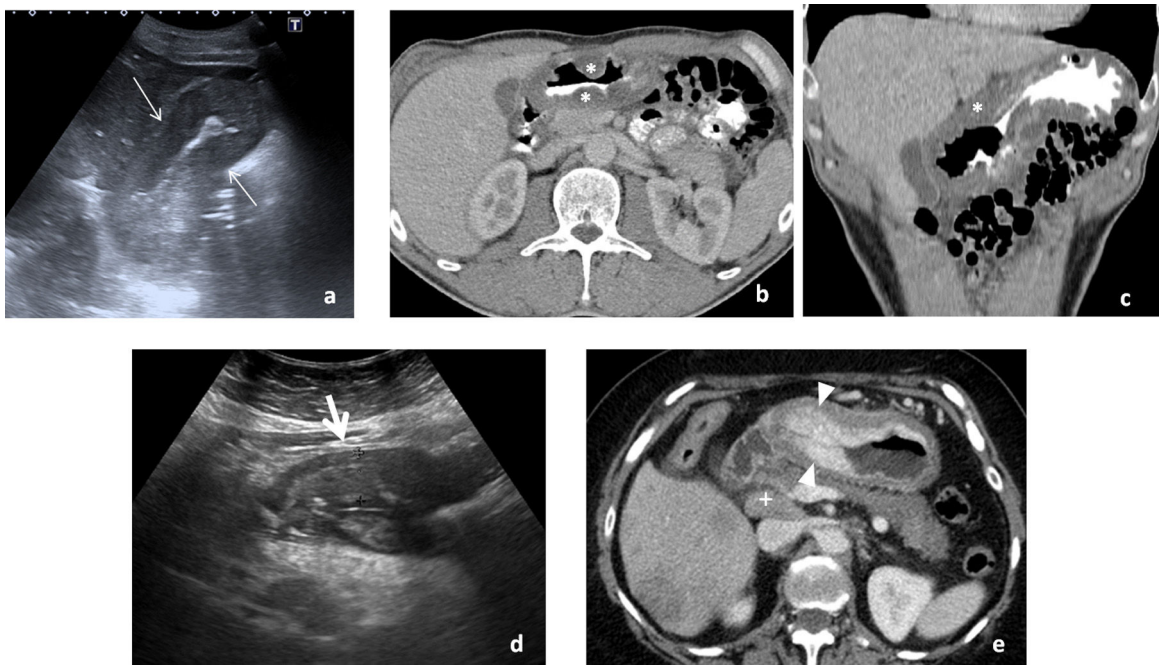


**Figure 1** Infectious diseases of the stomach. A–C) First case of a patient who came to Accident and Emergency with a history of severe epigastric pain, nausea and profuse vomiting for several hours, for which urgent ultrasound was requested (A). Circumferential and symmetric thickening (thin arrows) of the stomach wall in the body and antrum, which correlated with the subsequent axial computed tomography (CT) image (B) and coronal CT reconstruction (C), which showed a predominance of hypodense thickening (*) suggestive of submucosal oedema. Suspecting an inflammatory condition without being able to rule out other causes, an endoscopy was performed, showing thickening of gastric folds and mucosal erythema. Histology of the biopsy pointed to superficial chronic gastritis with eosinophilia, highly suggestive of gastritis due to Anisakis, although the parasite could not be identified. The condition resolved within a few days with symptomatic treatment. D and E) Second case of a patient reporting epigastric pain for several weeks with occasional vomiting. Ultrasound was requested initially, showing asymmetric thickening of the gastric antrum wall, more marked in the anterior wall (thick arrow), suspected of being of tumour origin (D). The subsequent CT scan (E) shows a similar finding, with irregular contrast uptake (arrowheads) by the gastric mucosa, with a prominent enlarged lymph node in front of the inferior vena cava (+) suggestive of lymph node spread. Endoscopy and biopsy confirmed the diagnosis of adenocarcinoma.

so we have to consider the diagnosis of lymphoproliferative syndrome, eosinophilic enteritis or Whipple's disease.[8]

**Strongyloides stercoralis**
Most common in tropical regions, it produces similar findings. Strongyloides stercoralis typically causes peripheral eosinophilia[9] and can lead to severe disseminated disease in immunosuppressed patients.[10]

**Mycobacterium avium intracellulare complex**
This should be considered in immunosuppressed patients, particularly in patients with HIV and CD4 lymphocyte levels <100/mL. It usually affects the jejunum, which appears thickened, but it can establish itself in any segment of the small bowel. It is accompanied by ascites and voluminous mesenteric and retroperitoneal lymphadenopathy, sometimes with a hypoechoic centre, similar to Whipple's disease. That finding may not be apparent due to the lack of immune response,6 in which case lymphoma cannot be ruled out. In disseminated forms, there may be lymphadenopathy in other chains (mediastinal or cervical) or lesions in solid organs (liver, spleen or kidneys).[11]

**Cryptosporidium**
Usually in patients with CD4 lymphocyte levels <50/mL. Involves the proximal small bowel, with no associated lymphadenopathy. It may be accompanied by cholangiopathy (bile duct dilation, distal common bile duct stenosis or acalculous cholecystitis), similar to CMV.

## Distal small bowel

Infections of the terminal ileum often spread to the caecum (Fig. 2). The main differential diagnosis is inflammatory bowel disease, usually indistinguishable in early stages (Table 2).

**Yersinia**
Along with *Salmonella* and *Campylobacter* it causes the majority of cases of self-limiting bacterial gastroenteritis. It is common in young patients and mimics appendicitis. Circumferential thickening of the terminal ileum, with regional lymphadenopathy and a normal appendix, is highly suggestive.[12] It may be accompanied by pharyngitis, arthritis and erythema nodosum.

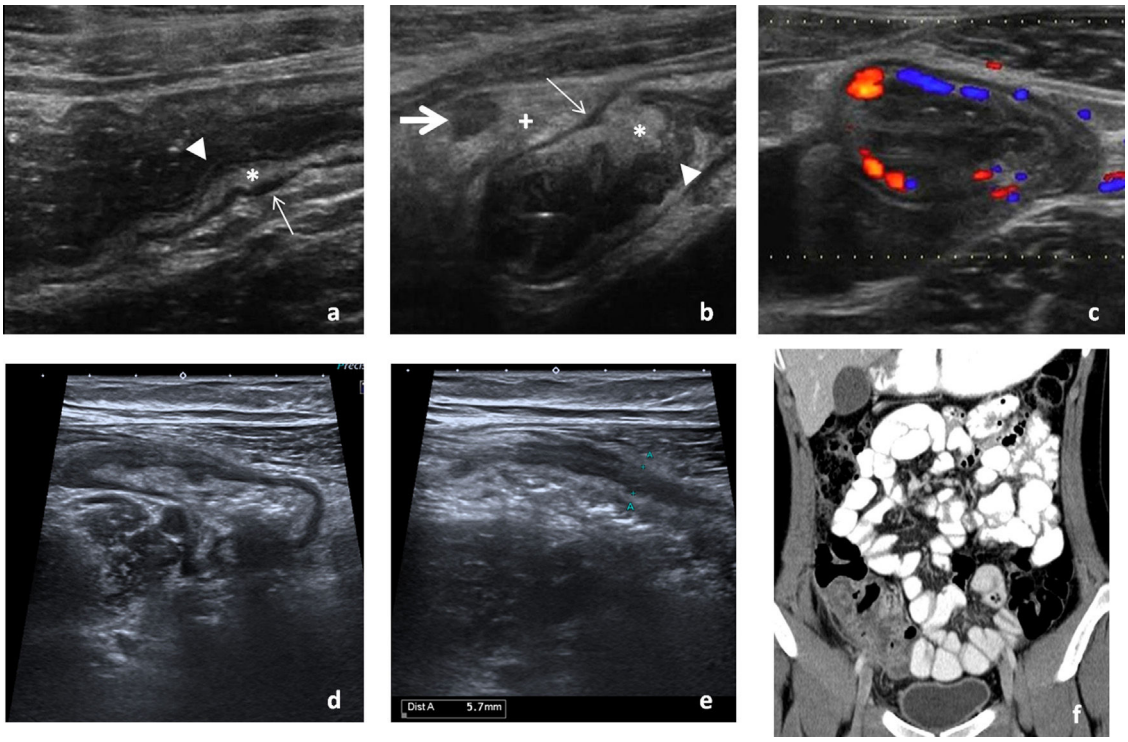


**Figure 2** Infectious diseases of the distal ileum. First case of a young patient with abdominal pain and diarrhoea who consulted Accident and Emergency. Ultrasound was performed to identify the origin of the symptoms. We present images in longitudinal section (A and B) of the terminal ileum, showing a thickening of the wall, but with preserved layer structure, affecting the mucosa (arrowheads) and submucosa (*), but not the muscle layer (thin arrows), characteristic of infectious enteritis as opposed to other causes of intestinal disorder. The colour Doppler study shows an increase in vascularisation secondary to the infection (C). Accompanying swelling can be seen, plus hyper-echogenicity of the adjacent mesenteric fat (+) and a reactive enlarged ileocolic lymph node (thick arrow). The stool culture came back positive for *Yersinia enterocolitica*. After antibiotic therapy and symptomatic treatment, the patient progressively improved until discharge. Second case of an 18-year-old patient who came to Accident and Emergency after several hours of low-grade fever and abdominal pain in the right iliac fossa. In the initial assessment, suspecting acute appendicitis, an ultrasound was performed, showing thickening of the terminal ileum wall extending to the caecum (D) and an ileocaecal appendix of normal lumen (E), suggesting an infectious disorder and ruling out the suspected appendicitis for which the scan was requested. At 24 h, an abdominal computed tomography scan was ordered. We are showing here a coronal reconstruction image from the study in the area of interest (F), which shows the same findings. Given the persistence of the symptoms, it was decided to operate on the patient, performing an ileocolic resection, with the histological result of suppurative enterocolitis with a normal appendix. The infectious agent that caused the condition could not be determined in the microbiological study.

**Salmonella**
This is more common in developed countries, being more serious in children and people with immunosuppression. Thickening of the mucosa with a feathery appearance has been described in ultrasound. Salmonella also affects the terminal ileum, with possible extension to the right colon which may be continuous or patchy, with local or regional lymphadenopathy and free fluid. In isolated cases, it may be complicated by gastrointestinal bleeding or perforation. In some cases, there may be acalculous cholecystitis or splenomegaly with possible abscess formation.[13]

**Campylobacter**
Tends to cause a self-limiting condition similar to the above. On rare occasions there may be extraintestinal involvement, such as cholecystitis, peritonitis, arthritis or myocarditis. *Campylobacter* has a well known relationship with Guillain-Barré syndrome.[14]

**Anisakis**
See Stomach section.

**Shigella**
See Left colon section.

## Distal ileum and caecum

### Tuberculosis

HIV infection and the use of immunosuppressants have increased the incidence of tuberculosis. The abdomen is a common site of extrapulmonary involvement. Clinically it presents with non-specific subacute symptoms of abdominal pain and constitutional syndrome with fever, vomiting and weight loss.

It can affect any section of the gastrointestinal tract, although the ileocaecal region is the usual location. It causes

**Table 2** Differential diagnosis of infectious enterocolitis. Other causes of diffuse bowel involvement.

| | |
|---|---|
| **Inflammatory causes** | |
| Inflammatory bowel disease | Particularly with Crohn's disease Asymmetric thickening of the terminal ileum, greater at the mesenteric border, with transmural involvement (including the muscle layer) and the presence of related complications (fistulas and abscesses). Ileocolic lymphadenopathy. Dilation pre-stricture |
| Coeliac disease | Thickening of the jejunum wall with diminished fold pattern and jejunisation of the ileum. Loop dilation with fluid content, increased peristalsis and intermittent intussusception. Prominent mesenteric ganglia. Splenic atrophy |
| Whipple disease | Chronic multi-systemic inflammation of bacterial origin. Thickening of the jejunal folds and characteristically hyperechoic mesenteric and retroperitoneal lymphadenopathy due to fat deposition. Hepatosplenomegaly and ascites. Spares the duodenum. Joint pains |
| Eosinophilic enteritis | Thickening of walls and folds of the gastric wall and of small bowel loops, with narrowing of the lumen, but preserving normal layer structure. No lymphadenopathy. Usually associated with peripheral eosinophilia. Where there is serous involvement, it is accompanied by exudative ascites (with eosinophils) and peritoneal nodules. Useful in assessing response to treatment (corticosteroids) |
| Vasculitis | Wall thickening with loss of stratification and focal dilation, most commonly affecting the small bowel. Vascular engorgement. Involvement of other organs (genitourinary, liver, skin) |
| **Iatrogenic causes** | |
| Chemotherapy | Conventional chemotherapy: enteritis with wall thickening affecting the mucosa and submucosa. Molecular therapy: pneumatosis, perforation, enteritis and colitis |
| Radiotherapy | Thickening of the intestinal loops in the pelvic region and lower abdomen corresponding to the irradiation field (pelvic cancer the most commonly treated with radiotherapy), initially due to oedema which evolves to fibrosis. Can cause strictures |
| Neutropenic colitis (typhlitis) | Patients with severe neutropenia usually due to cancer treatment. Thickening of the wall of the caecum (may extend to the ileum and ascending colon). Moderate involvement of the pericaecal tissue, little ascites and not usually accompanied by lymphadenopathy. Can be complicated by abscess and perforation. High mortality rate (50%) |
| Graft versus host disease (GVHD) | Patients who have received a haematopoietic stem cell transplantation. *Acute form* (30-100 days post-transplantation): abdominal pain and secretory diarrhoea, with patchy involvement of bowel loops, which show wall oedema and distension of the lumen with fluid content. *Chronic form* (>100 days post-transplant): malabsorption syndrome, not usually with any signs in imaging tests |
| **Vascular causes** | |
| Ischaemic bowel | Wall thickening with absence of flow in Doppler study in the acute phase. The thrombus may be visualised within the vessel lumen. Distribution according to the territory involved (superior or inferior mesenteric artery). Ultrasound has a very limited role in this disorder. CT is the test of choice. |
| **Cancer-related causes** | |
| Lymphoma | Most often affects the stomach and small bowel. Circumferential thickening with loss of stratification and marked wall thickening, but without causing obstruction. Accompanied by lymphadenopathy. |
| Others (GIST, carcinoma or metastasis) | The wall thickening tends to be more prominent, asymmetric, affecting a short segment, with loss of the wall stratification, but with no accompanying alteration of the adjacent fatty tissue or ascites |

concentric thickening of a short segment of the wall, sometimes multifocal, and initially, slight narrowing of the lumen which can later lead to obstruction. Thickening of the ileocaecal valve and the medial wall of the caecum is typical. Although uncommon, it can be complicated by perforation or fistulous tracts.

It is accompanied by mesenteric, periportal and superior para-aortic lymphadenopathy, often with a hypoechoic centre due to necrosis (Fig. 3A), and occasionally calcified (not generally in the active phase). They are less likely than other conditions to form clusters.

Diagnosis is guided by the presence of microabscesses in the liver and spleen (Fig. 3B), and the involvement of other abdominal organs (adrenal glands, pancreas or genitourinary system) and very often sites outside the abdomen, such as the lungs, bones or central nervous system.[6,15–19]

## Right colon

### Entamoeba histolytica

Endemic in tropical and subtropical regions and in travellers or immigrants from those territories. It is usually asymptomatic, but can cause an invasive condition. It mainly affects the caecum and, unlike tuberculosis or Crohn's disease, does not involve the ileum. The wall thickening can mimic a cancer lesion (amoeboma). The rectum may also be affected and some patients may develop a liver abscess, generally unilocular with fine echogenic content, which can help pinpoint the diagnosis. Other abscesses in the brain, heart and lungs are very rare.[3,20,21]

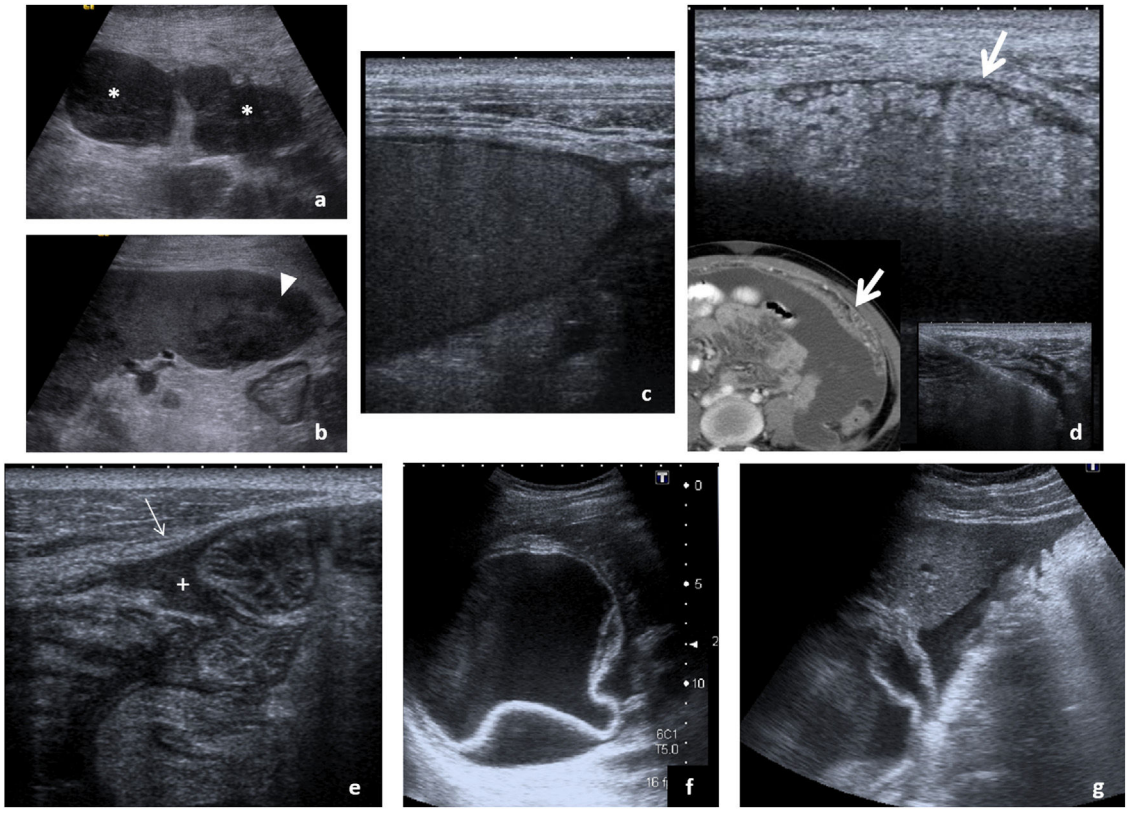


**Figure 3** Infectious diseases of the peritoneum. A–D) Typical findings of tuberculous peritonitis in various patients. Mesenteric lymphadenopathy (A) with a hypoechoic centre due to the presence of necrosis (*), splenic involvement (B) with abscess in the lower pole of the spleen (arrowhead) and ascites (C) with echogenic stippling due to dense material. A significant finding was the thickening of the greater omentum (thick arrows), which can be seen in detail on the ultrasound image (D), and is correlated with the tomographic image shown in the bottom left corner. This raises the differential diagnosis with tumour invasion, so usually requires a histological study after obtaining a sample; which may be ultrasound-guided, as shown in the bottom right corner image. E–G) Peritonitis of other origin. In the first case (E), a patient with acute appendicitis accompanied by a small amount of free fluid between loops, with echogenic stippling (+) and linear thickening of the parietal peritoneum (thin arrow), which suggests the presence of associated focal peritonitis. The second case was parasitic peritonitis in a patient with a hepatic hydatid cyst (F) with folded membranes and the presence of perihepatic fluid (G) suggesting that it has become complicated, with rupture and spread of the contents into the peritoneum.

## Left colon

### Shigella

A group of highly contagious Gram-negative bacteria whose only reservoir is humans. It causes dysentery in less developed countries, with blood and mucus in the stool. The differential diagnosis is with other microorganisms, such as enterohaemorrhagic *E. coli*, *Salmonella*, *Yersinia*, *Campylobacter*, amoebiasis and *Clostridium difficile*. Shigella typically affects the descending and sigmoid colons, with thickening of the wall and mucosal ulcers. Sometimes it becomes established in the distal ileum. It can be associated with haemolytic uraemic syndrome in children under five years of age and reactive arthritis in adults.[22,23]

## Rectum and sigmoid colon

Herpesviruses, gonorrhoea, and chlamydia are a group of pathogens which cause sexually transmitted infection and present with symptoms of proctitis (abdominal pain, diarrhoea, rectal bleeding, purulent discharge and tenesmus). The main differential diagnosis is inflammatory bowel disease. They are usually accompanied by purulent urethral discharge. The presence of enlarged femoral lymph glands, sometimes abscessed, suggests *Chlamydia* lymphogranuloma venereum, while vesicles in the perianal region suggest herpesvirus.[24] Ultrasound has a very limited role in these situations.

## Pancolitis

### Clostridium difficile

The incidence and severity of *Clostridium difficile* is increasing due to the use of broad spectrum antibiotics. Although not exclusive and it may not occur, very marked thickening of the wall of the entire colon is highly suggestive. However, there may only be segmental involvement and diagnosis is confirmed by the detection of toxins in fae-

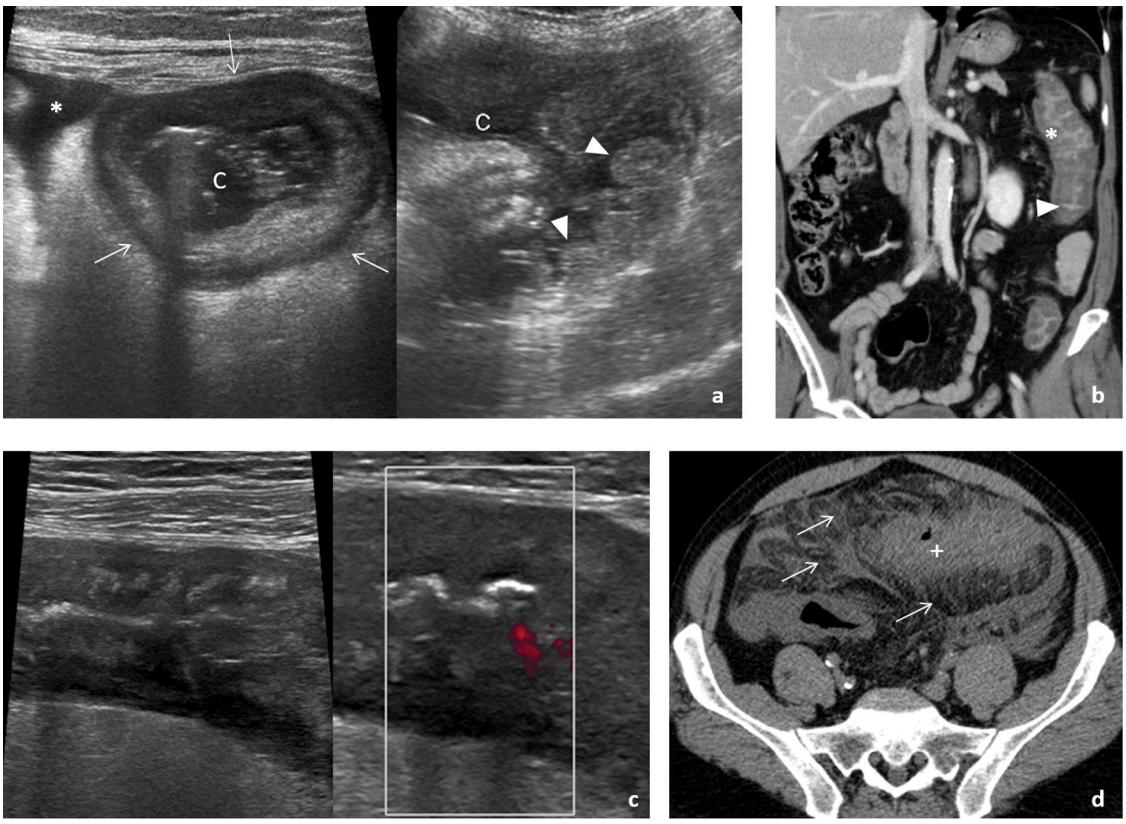


**Figure 4** Infectious diseases of the colon. A and B) Pseudomembranous colitis. A) Ultrasound images in a patient with bloody diarrhoea showing a colon (c) with marked wall thickening (arrows) and prominent and irregular internal mucosal folds (arrowheads). There is mild ascites (*). B) Coronal reconstruction from a computed tomography (CT) study in another patient with the same diagnosis, where we can see significant thickening of the wall of the left colon, with a predominance of oedema in the submucosal layer (*) and enhancement of the mucosa (arrowhead), with minimal involvement of the adjacent mesentery, characteristic in this disease. C and D) Ischaemic colitis. Ultrasound images (C) showing the abnormally thickened wall of the left colon with loss of normal stratification. In the Doppler study, it was not possible to detect the presence of flow inside despite using colour Power or Power Doppler, which is much more sensitive to the detection of slow flow. In the axial image of the CT scan (D), performed without contrast due to deterioration in the patient's renal function, we see the thickening of the wall of the sigmoid colon (+), which is accompanied by significant mesenteric fat stranding (thin arrows ), findings which usually appear in the reperfusion phase after occlusive or non-occlusive mesenteric ischaemia. Fig. 4 a courtesy of Dr T. Ripollés (Valencia, Spain).

ces and stool culture. Small bowel involvement has been described. Ultrasound shows an increase in the thickness of the submucosal layer (hyperechoic), with normal thickness of the muscle layer (hypoechoic) (Fig. 4). Hyperechoic images have been reported in the lumen which may indicate the presence of membranes. Pericolonic involvement is disproportionately rare. It is very often accompanied by ascites.[25] It can progress to toxic megacolon with high morbidity and mortality rates.

## Cytomegalovirus

In immunosuppressed patients, cytomegalovirus usually causes diffuse colitis, although cases of segmental involvement of the colon or the ileocolic region have been described, with thickening of the wall and pericolic fat stranding in all cases, and the possibility of ascites. It is not usually accompanied by lymphadenopathy, but is sometimes associated with cholangiopathy. A high degree of suspicion is necessary to make the diagnosis (inclusion bodies in biopsy) and to start treatment with antivirals at an early stage, to avoid complications such as ischaemia or perforation.[3,26]

.

## Escherichia coli

Enterotoxigenic strains, responsible for traveller's diarrhoea, cause milder symptoms. Enterohaemorrhagic strains, from eating meat in poor condition and probably underdiagnosed, like other pathogens, can cause severe dysentery in the elderly and children. It causes pancolitis, although with greater involvement of the right colon. Like *Shigella*, it can trigger haemolytic uraemic syndrome.[22,27]

The differential diagnosis of bowel infections includes other symptoms of acute abdomen of intestinal origin (appendicitis, diverticulitis, adenitis, etc), already discussed in another article in this series, and in particular, other causes of diffuse bowel involvement of an inflammatory, iatrogenic, vascular or cancer-related nature (Table 2).[28–31]

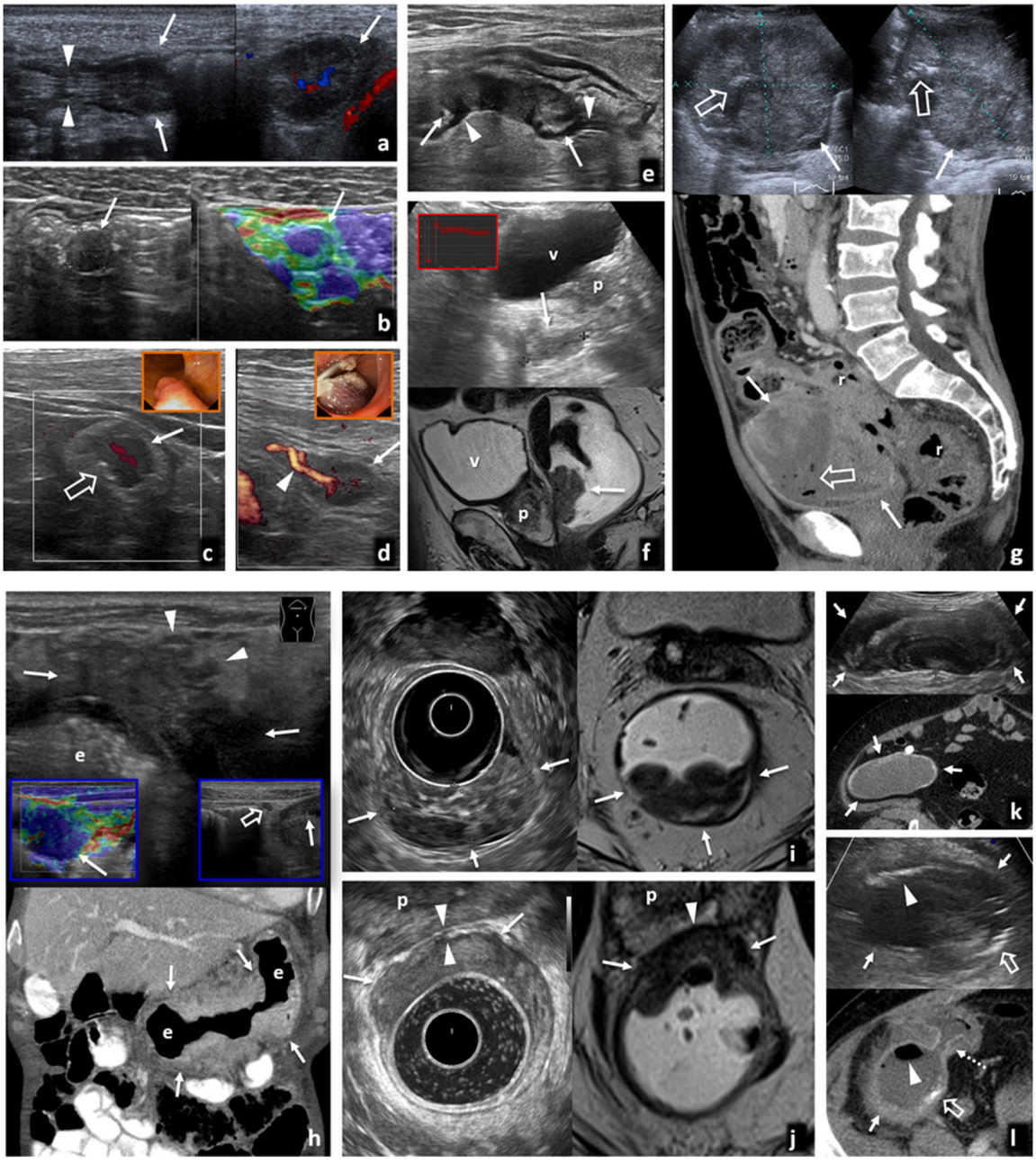


**Figure 5** Polyps and carcinomas. A) hypoechoic adenomatous polyp 13 mm in size (arrows) in the lumen of the transverse colon, with a pedicle that follows the layered structure of the wall (arrowheads) and flow demonstrated on Doppler (right). Incidental finding in 77-year-old male. B) Hypoechoic adenomatous polyp (arrows) in the sigmoid colon, an incidental finding in a 44-year-old male. Image stability over time and tissue stiffness, with blue tones in the qualitative pressure or strain elastography image (right), confirm the finding. C) Haggitt 1 carcinoma on a 15-mm hypoechoic adenomatous polyp (arrow) in the lumen of the distal left colon, with a vessel inside it on Doppler and a small superficial ulceration (empty arrow). Incidental finding on ultrasound for atheromatosis in a 67-year-old male. Inset, colonoscopy image prior to resection. D) Haggitt 1 carcinoma on a 20-mm hypoechoic adenomatous polyp (arrow) in the lumen of the sigmoid colon, with a vessel in its pedicle on Doppler (arrowhead). Incidental finding in study for nonspecific abdominal discomfort in a 78-year-old female. Inset, image during endoscopic resection. E) Infiltrating adenocarcinoma of the sigmoid colon T2 N0 M0 on ultrasound due to anaemia in an 85-year-old male with multiple comorbidities. Infiltrating hypoechoic thickening with retraction of the posterior wall of the colon (arrows), without going beyond the hypoechoic muscularis propria layer (arrowheads). Ultrasound was more accurate than computed tomography (CT) (not shown) in local/regional staging in this case, allowing a rapid and limited laparoscopic surgical approach in a clinically complex patient. F) Polypoid carcinoma in the lower rectum, ultrasound finding using the bladder (b) as an acoustic window. Hypoechoic nodular lesion (arrows) measuring 33 mm. Inset, time-intensity curve of ultrasound with contrast to confirm the finding (video 1). p: prostate. Bottom image: correlation in T2-weighted sagittal magnetic resonance imaging (MRI) with endorectal gel for local/regional staging. G) Colorectal transitional cell carcinoma as an ulcerated, necrotic exophytic mass mimicking a GIST. Top image: ultrasound,

## Peritoneum

*Tuberculous peritonitis* is the most common manifestation of abdominal tuberculosis. Classically, it is divided into three patterns: *wet peritonitis*, the most common (90%), with freely distributed or loculated ascites, echogenic stippling due to high fluid density and peritoneal thickening (Fig. 3C); *dry peritonitis*, with little fluid and complete or incomplete adhesions; and *fibrotic-fixed peritonitis*, with mesenteric nodules and masses and nodular thickening of the omentum. Ultrasound enables detailed examination and serves as a guide for diagnostic biopsy (Fig. 3D). Described as the great mimic, differential diagnosis includes peritoneal carcinomatosis, lymphoma, Crohn's disease, mesothelioma, pseudomyxoma peritonei and pyogenic peritonitis.

*Pyogenic peritonitis* (Fig. 3E) is the result of complication of an abdominal infection generally of intestinal origin and can lead to abscesses, which often require ultrasound-guided percutaneous drainage. *Spontaneous bacterial peritonitis* is a complication of decompensated cirrhosis, and should be suspected in cases of ascites with fever or clinical deterioration. Diagnosis requires ultrasound-guided diagnostic paracentesis. We should also mention *parasitic peritonitis*, which in our setting is usually caused by the rupture of a hydatid cyst of the liver (Fig. 3F and G).[32,33]

## Neoplastic diseases of the bowel and peritoneum

Ultrasound only plays a very small role in clinical guidelines for the detection and staging of gastrointestinal and peritoneal neoplasms. Only transrectal ultrasound (TRUS) is comparable, in some cases, to magnetic resonance imaging (MRI) in local-regional staging of rectal cancer.[34] However, it is the most common technique for nonspecific symptoms, and so provides the opportunity to detect and begin investigation of such tumours, some of which may in fact be found incidentally.[35,36] Despite its known limitations, it is safe, cheap, dynamic and interactive, it provides high spatial resolution in accessible areas and has numerous added technical resources (gradual compression, high-resolution probes, Doppler, intravenous or oral contrast, elastography, transrectal or transvaginal access, etc).[2,28,29,37] Any abdominal-pelvic ultrasound examination should reserve a few minutes for the systematic study of the gastrointestinal tract and peritoneal structures; the technical possibilities are either detailed in another article in this series or will be discussed later, but without addressing endoscopic ultrasound, not part of a radiologist's remit, which is generally limited to proximal or distal areas of the gastrointestinal tract.[38–40]

Gastrointestinal neoplasms generally appear as a solid mass or a short segment (<10 cm) with marked hypoechoic asymmetric wall thickening (>12 mm) with disruption of the layer structure.[29] Some lymphomas or incipient tumours may preserve the layer structure, while it may also de disrupted in ischaemic or inflammatory conditions with transmural involvement. The ultrasound pattern, topography and clinical context help narrow the differential diagnosis and occasionally provide exclusive information. Table 3 . shows a summary of the most relevant features.

We discuss gastrointestinal neoplasms with a nosological pattern, reserving one chapter for those of the peritoneum and another to discuss the role of ultrasound as a guide to percutaneous biopsy.

## Polypoid lesions (Fig. 5A–D)

There is evidence of a gastrointestinal polyp-cancer sequence, with stepwise models (succession of mutations or epigenetic alterations), big bang (massive episodes in ini-

transverse (left) and longitudinal (right) sections over the hypogastrium. Heterogeneous hypoechoic mass (arrows) due to necrosis, with gas foci (empty arrows) due to ulceration. Bottom image: sagittal CT. The mass is in contact with the anterior aspect of the rectosigmoid junction (r). GIST was suspected, but it corresponded to an adenocarcinoma with an unusual pattern of presentation. H) Gastric adenocarcinoma T4a N2 M0. Top image: ultrasound for constitutional syndrome in an 83-year-old male. Marked and irregular hypoechoic thickening of the stomach wall (st: gastric lumen), with ulcerations (not shown) and clear nodular spread to the fat of the gastrocolic ligament (arrowheads). Elastography (bottom left inset) shows marked tissue stiffness. Regional lymphadenopathy can also be seen (empty arrow in bottom right inset). Bottom image: coronal CT in portal phase. The extreme thinness of the patient made staging less accurate than with ultrasound. I) T1 rectal adenocarcinoma on hairy polyp (arrows) in a 67-year-old male. Endorectal ultrasound (left) shows a polypoid lesion of intermediate echogenicity, defining the integrity of the muscularis propria layer (hypoechoic) with more precision than MRI (right: transverse T2-weighted with endorectal gel), enabling transanal resection. J) Superficial T3a inferior rectal adenocarcinoma in a 72-year-old male. Endorectal ultrasound (left) precisely shows an eccentric hypoechoic thickening in the anterior aspect of the lower rectum, transgressing the hypoechoic muscularis propria layer with superficial nodulations (arrows), confirming superficial T3 extension. Shows preservation of a fatty plane (arrowheads) with the prostate (p). Transverse T2-weighted MRI (right) raises doubts in this case from T2 to T4b due to prostate invasion. K) Appendiceal mucocele. Top image: incidental ultrasound finding in a 77-year-old female with acute calculous cholecystitis. Ovoid mass with internal layered structure with alternating echogenicities (characteristic önion skinp̈attern) in the right iliac fossa (arrows). Bottom image: axial CT shows fine wall calcifications, but is not able to demonstrate the mucinous structure of the cystic lesion with the precision of ultrasound. L) Appendiceal mucocele with superinfection in contact with the caecum. Top image: ultrasound in a 62-year-old male with abdominal pain and fever. Heterogeneous cystic mass in the right iliac fossa (arrow), with echogenic foci representing gas (arrowhead) and wall calcifications (empty arrow). Bottom image: CT also demonstrates communication of the mucocele with the lumen of the caecum (broken arrow).

**Table 3** Summary of the features of the four main types of primary gastrointestinal malignant neoplasms.

| Tumour subtype | Wall layer | General features | Stomach | Small bowel | Colon | Rectum | General ultrasound signs |
|---|---|---|---|---|---|---|---|
| Adenocarcinomas | Mucosa | Most common GI cancer | 13% 90% | 2% 32% | 60% > 97% | 25% > 97% | Hypoechoic heterogeneous. Destroys layers |
| | | Age >55 except in hereditary syndromes | 4th cancer | D > J > I | 3rd cancer | 3rd cancer | Infiltrating wall thickening (mass less common) |
| | | | 2nd mort. | | 3rd mort. | 3rd mort. | Eccentric, short, stricturing |
| | | | | | | | Ulcerations, perforation |
| | | | | | | | Moderate lymphadenopathy |
| | | | | | | | Liver and peritoneal metastases (carcinomatosis) |
| | | | | | | | Moderate vascularisation |
| Neuroendocrine tumours | Deep submucosa | 2/3 of NET are GI | 5% 1% | 60% 43% | 15% <1% | 20% 1% | Hypoechoic nodule (±hyper halo) wall-lumen |
| | | Younger in general | | I > J > D | Appendix | | Bowel retraction |
| | | | | | | | Desmoplastic mesenteric lymphadenopathy is dominant |
| | | | | | | | Liver and peritoneal metastases (nodular) |
| | | | | | | | Hypervascular |
| | | | | | | | Typo III gastric: aggressive. Mimic adenocarcinomas |
| | | | | | | | Appendiceal: common incidental finding |
| Lymphoma | Mucosa-submucosa | GI tract: extranodal most common | 65% 3% | 30% 8% | 3% <1% | 2% <1% | Mass, marked hypoechoic wall thickening |
| | | 1–4% of primary GI malignant tumours | | D ≈ J ≈ I | | | Occasionally partial preservation of layers |
| | | NHL 10% initial GI involvement. 60% advanced | | 75% Near | | | Relatively long, not obstructive |
| | | Diffuse large B-cell NHL most common | | East | | | Ulceration, cavitation, aneurysmal dilation |
| | | | | | | | Prominent enlarged lymph nodes |
| | | | | | | | Involvement of spleen, peritoneum or other organs |
| | | | | | | | Hypovascular |
| GIST | Muscularis propria | 1% of GI malignant tumours diagnosed | 65% 6% | 30% 17% | 3% 1% | 2% <1% | Hypoechoic mass with exophytic growth |
| | | Up to 30% gastric 1–10 mm in post-mortem examinations | | D ≈ J ≈ I | | | Large: heterogeneous (necrosis, cysts) |
| | | Mean age: 64. Less in syndromes | | | | | Tend to ulcerate and cause intestinal and peritoneal bleeding |
| | | | | | | | Lymphadenopathy rare |
| | | | | | | | Liver and peritoneal metastases (nodular) |
| | | | | | | | Hypervascular |

D: duodenum; I: ileum; GI: gastrointestinal; GIST: gastrointestinal stromal tumour; NHL: non-Hodgkin's lymphoma; NET: neuroendocrine tumour; J: jejunum.
In the boxes for topographic involvement, the percentage on the left refers to the proportion of tumours of that subtype of primary malignant tumour (out of all gastrointestinal) which affect that specific location. The percentage on the right tells us what proportion of all primary malignancies in that location those of that particular subtype represent. For example, 60% of gastrointestinal NET affect the small bowel, where they represent 43% of all primary malignancies. These figures are approximate, with the averages taken and numbers rounded by the authors from various sources.

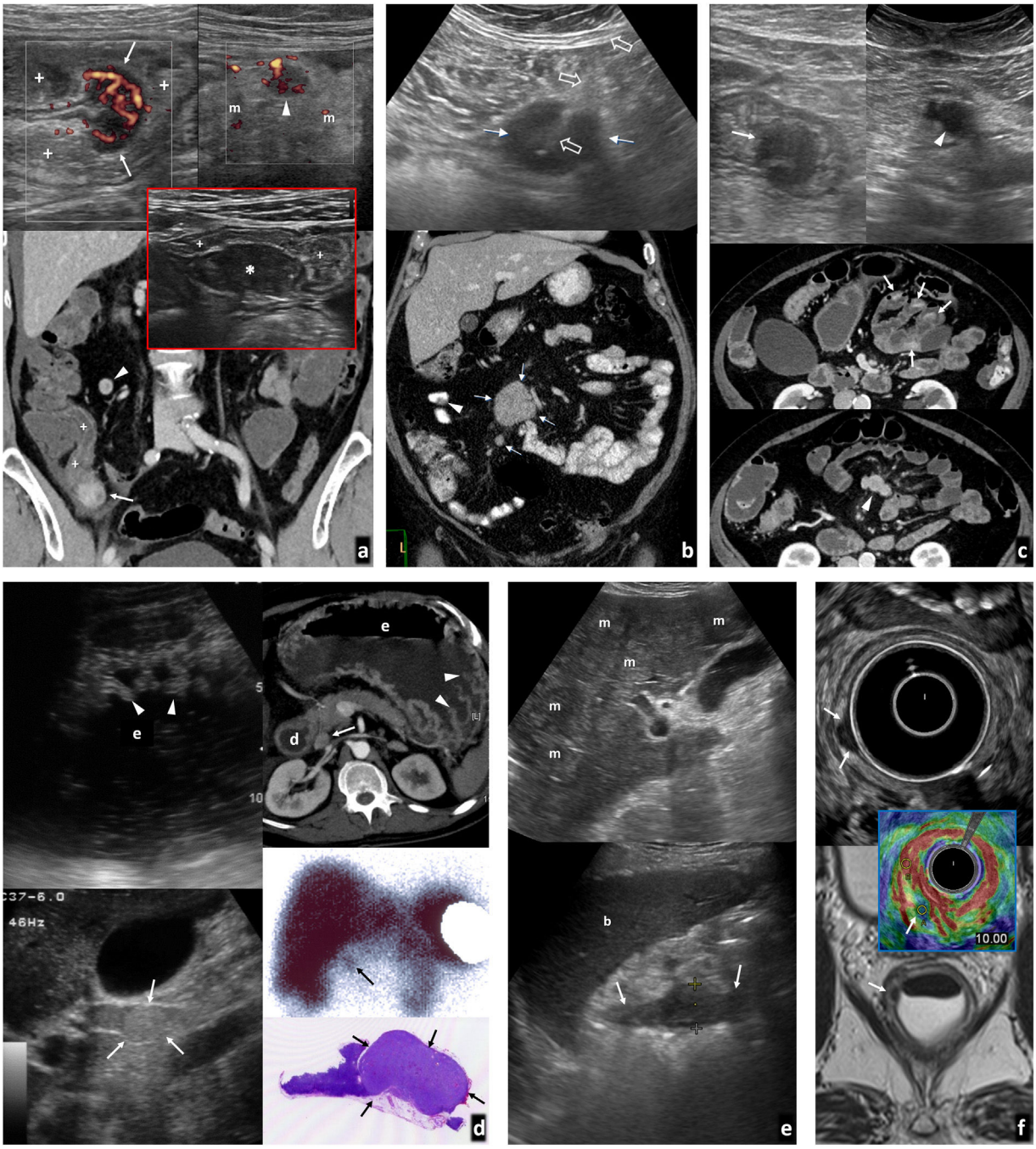


**Figure 6** Neuroendocrine tumours. A) Terminal ileum carcinoid tumour. 62-year-old female with vomiting and abdominal pain. History of surgery for pituitary macroadenoma. Top image: ultrasound. Bottom image: coronal computed tomography (CT). Hypoechoic nodular lesion with abundant vascularisation on Doppler and CT (arrows), in the internal angle of the folded section of the distal ileum (+), with ineffective peristalsis in real time (video 2). Also, hypoechoic and vascularised lymphadenopathy (arrowheads) in swollen and echogenic regional mesocolon (m). Diagnosis made of multiple endocrine neoplasia-1 (MEN-1). Inset: endometrial implant (*) in the terminal ileum (+) in another patient, seen as a hypoechoic nodule infiltrating the serosa, retracting the loop, but not affecting the deep layers, showing similar findings, with which a differential diagnosis had to be made (not vascularised and without lymphadenopathy in this case). B) Ileal carcinoid only showing as a mesenteric mass. Top image: ultrasound-guided percutaneous biopsy (empty arrows) of a hypoechoic mesenteric nodule (arrow), which showed lymph node metastasis from a neuroendocrine tumour. Bottom image: coronal CT scan with oral and intravenous contrast. Mesenteric lymphadenopathy nodules (arrows). A primary intestinal millimetric carcinoid was identified during surgery and, retrospectively, could correspond to the small filling defect indicated by the arrowhead. C) Multiple jejunal carcinoids and mesenteric lymph node metastases. 71-year-old female with nonspecific abdominal discomfort. Top images: ultrasound scans. Middle and bottom: axial CT-enterography images in two different planes. Five hypoechoic, hypervascular tumours (one not shown) were detected in folded sections of the jejunum (arrows), with a small cluster of enlarged lymph nodes, also hypervascular and hypoechoic at the tributary mesenteric vein

tial phases) or of punctuated equilibrium (periods of great transformation alternating with phases of stasis or gradual changes).[41] A conservative approach is accepted for tiny (<5 mm) and small (6—9 mm) polyps, with negligible risk of dysplasia or cancer. Cancer is detected in 1% of adenomatous polyps measuring 1—2 cm and in 50% of those larger than 3 cm. The flat serrated polyps, typical of the right colon, are less aggressive than was classically thought Fig. 5 Ultrasound can identify large colon polyps (>1 cm), preventing or facilitating the early detection of cancer, with a specificity of 94.4%, a sensitivity of 28.6% without preparation[42] and 91% with hydrocolonic sonography[43] in adults. In children with symptoms, it achieves a sensitivity of 47% and a specificity of 100% without preparation[44] and 95% and 100% respectively with glycerine enema.[45] They are more accessible in the left and sigmoid colon and less in the rectum and splenic flexure. They are also detectable outside the colon.[46,47] They appear as persistent endoluminal hypoechoic nodular lesions, occasionally with a pedicle that shows continuity with the wall layers. Detection of small cystic foci, vascularisation with Doppler or contrast and elastography, along with a thorough examination, help differentiate them from faeces, haustra or the taeniae coli. Size, deep infiltration into the wall, and ulceration are correlated with malignancy.[48] There are reports of laparoscopic ultrasound with saline enema being useful in intraoperative detection of polyps, with some advantages over tattooing with India ink.[49,50]

## Carcinoma (Fig. 5E-L, video 1)

When it is not polypoid, it usually behaves as asymmetric, eccentric or concentric hypoechoic wall thickening in a short segment of gastrointestinal tract, with abrupt edges and loss of stratification.[29,35,36] Rarely, it appears as an exophytic mass, mimicking a gastrointestinal stromal tumour (GIST). Ulcerations (intratumoural gas foci), stiffness, stricture (fixed lumen and ineffective proximal peristalsis), and moderate regional lymph node involvement are common. Experience and thorough examination (which should be even more diligent if there is a high degree of suspicion or liver metastases) facilitate detection in difficult regions.

Several articles show diagnostic values above 80% for gastric and colon carcinomas taking endoscopy as a reference,[51,52] better if the rectum is excluded. One study showed a moderate (64%) coincidence with the histological T-stage in colon cancer, which rose to 89% (good), establishing groups with interest for surgical planning and prognosis.[52] Hydrocolonic sonography achieves better results than CT,[53] but interest has progressively waned due to poor tolerance. Chinese authors achieved good results in the detection and characterisation of carcinoma and other gastric lesions[46,47] using a double contrast technique (intravenous and oral derived from rice and soy, of intermediate consistency and echogenicity, with good transmission, not available in our environment).

TRUS can surpass MRI in the T1-T2 stage (selecting candidates for endoscopic or transanal resection), T2-T3 superficial and T3 superficial/deep (selecting candidates for neoadjuvant treatment).[34] It requires experience and is less useful in T4 and N.

An appendiceal mucocele is the accumulation of mucin, with different echogenicities, sometimes alternating (önion skin sign¨), in the lumen of a distended appendix (>15 mm), occasionally with gas (due to superinfection and/or communication with the caecal lumen) or wall calcification. An irregular wall or solid nodules should suggest an underlying cystadenocarcinoma. Perforation can lead to pseudomyxoma peritonei.[35,54]

## Neuroendocrine tumours (NET) (Fig. 6, video 2)

Gastrointestinal NET generally form in the submucosal layer. The World Health Organisation (WHO) considers them potentially malignant, establishing three grades of aggressiveness according to cell proliferation. Within the G3 group, tumours with Ki-67 > 50 are carcinomas. They can occur in genetic syndromes (MEN-1, von-Hippel-Lindau, tuberous sclerosis and neurofibromatosis-1). Many secrete hormones or amines, which determine signs and symptoms and facilitate analytical detection (serotonin or its derivatives, chromogranin-A, gastrin, synaptophysin, neuron specific enolase, etc.) or detection with nuclear medicine procedures (particularly $^{68}$Ga- DOTATATE PET-CT due to the expression of the SSTR2 receptor in differentiated tumours, with $^{18}$FDG PET-CT used to assess metabolic activity in undifferentiated lesions)[55–57] Fig. 6 The most common NET are

(arrowheads). D) Zollinger-Ellison syndrome due to type II neuroendocrine tumour (gastrinoma) of the upper gastrointestinal tract. 44-year-old male with vomiting, diarrhoea and shock. Left image: ultrasound. Top right image: axial CT. Copious amounts of fluid in the stomach (st), duodenum (d), and proximal jejunum (not shown), with marked thickening of the gastric folds (arrow heads). Medial to the duodenum and posterior to the pancreas, a hypervascular and slightly echogenic nodule (arrows) can be seen within a nodal structure. This region is within the so-called g̈astrinoma triangle.¨ Right centre: octreotide scan. Uptake by the nodule is confirmed (arrow). There is also hypergastrinaemia. Bottom right: surgical specimen of the gastrinoma (arrows) within a lymph node. E) Type III gastric neuroendocrine carcinoma. 59-year-old male with constitutional syndrome. Ultrasound shows extensive liver metastases (m) and, using the spleen (sp) as an acoustic window, an invasive tumour in the greater curvature of the stomach. Adenocarcinoma was suspected, but endoscopic biopsy showed neuroendocrine carcinoma. F) Rectal neuroendocrine tumour. Colonoscopy finding after a positive faecal occult blood test in a 62-year-old male. Top image: transrectal ultrasound. Bottom image: T2-weighted axial MRI. Tumour measuring 7 × 5 mm (arrows) with hypoechoic and hypointense behaviour on T2-weighted images, located in the deep part of the submucosal layer of the lower rectum, with moderate tissue stiffness on elastography (central inset), with a strain ratio of 10 with respect to the normal rectal wall. A transanal endoscopic resection was performed.

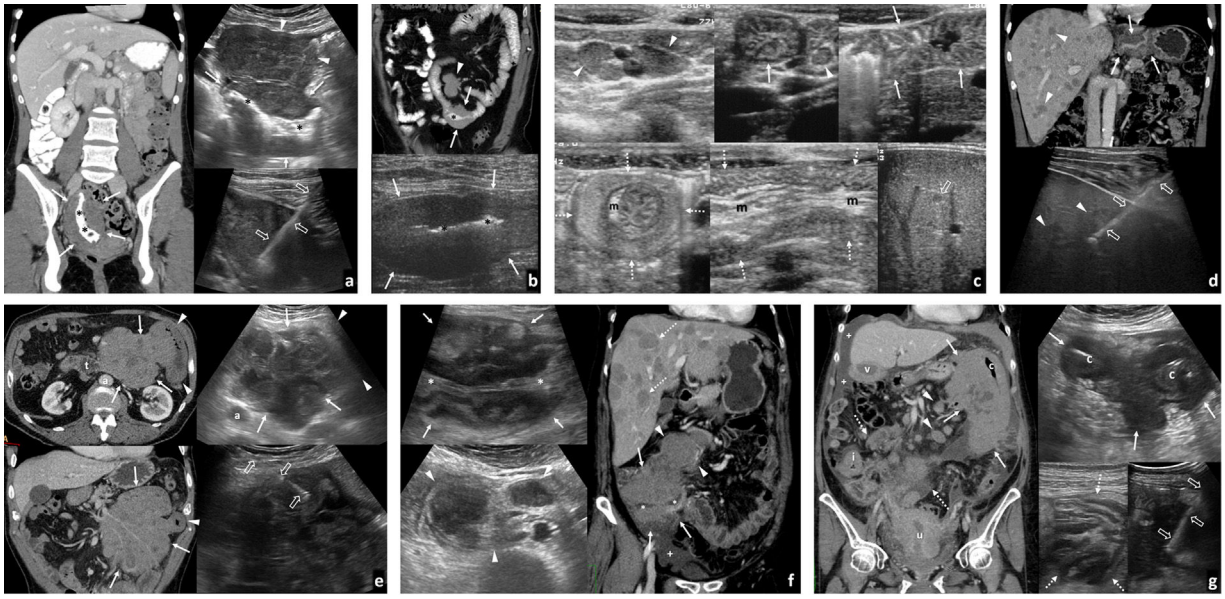

**Figure 7** Gastrointestinal lymphomas. A) Diffuse large-cell lymphoma of the terminal ileum. 36-year-old female. Left image: coronal computed tomography (CT) with oral and intravenous contrast. Right image: ultrasound. Marked hypoechoic and hypovascular wall thickening in a long stretch of the distal ileum (arrows) with dilated lumen (*). Accompanied by an adjacent mesenteric mass of similar echogenicity (arrowheads), on which ultrasound-guided core needle biopsy (CNB) was performed (empty arrows). A) Diffuse large-cell lymphoma of the distal jejunum. 70-year-old male. Top image: coronal CT scan with oral and intravenous contrast. Bottom image: ultrasound. Marked hypoechoic and hypovascular wall thickening in a shorter stretch of the distal jejunum (arrows), also with aneurysmal dilation (*) and an accompanying mass of mesenteric lymphadenopathy (arrowhead). The diagnosis was made from percutaneous biopsy of the bowel thickening (not shown). C) Immunoproliferative small intestinal disease (or Mediterranean lymphoma, subtype of extranodal marginal zone lymphoma). 17-year-old male with diarrhoea, fever and abdominal pain. Ultrasound shows homogeneous mesenteric lymphadenopathy (arrowheads), thickening of the folds of the proximal jejunum (arrows), with a long intussusception of the jejunum (discontinuous arrows) with mesentery inside (m), as well as small focal hypoechoic hepatic lesions (empty arrows). The diagnosis was obtained with the biopsy of two focal liver lesions (not shown). D) High-grade gastric enteropathy-associated T-cell lymphoma. 61-year-old male with a diagnosis of coeliac disease. Top image: CT. Bottom image: ultrasound-guided core needle biopsy (CNB). Hypovascular and hypoechoic (not shown) circumferential thickening of the antrum of the stomach (arrows), with multiple focal low-uptake (arrowheads) and mildly hypoechoic liver lesions. Gastroscopy shows an ulcerated antral lesion, but biopsies were repeatedly negative. Diagnosis was achieved from percutaneous biopsy of the liver lesions. E) Low-grade follicular lymphoma of the proximal jejunum. 73-year-old male. Left image: axial CT (upper) and thin coronal maximum intensity projection (MIP) (lower). Right image: ultrasound, transverse section (top) and percutaneous biopsy. Eccentric wall thickening of a section of the proximal jejunum (arrowheads) with a large mesenteric mass (arrows) extending up to the angle of Treitz (t), with little mass effect on the mesenteric vessels through it. a: aorta. The heterogeneity of this lymphadenopathy cluster is better defined on ultrasound, enabling guiding of the percutaneous biopsy to the most solid part of the mesenteric mass (hollow arrows). The patient remains in complete remission three years after starting chemotherapy. F) Ileocaecal Burkitt's lymphoma. 46-year-old female. Left image: ultrasound. Right image: coronal CT. Significant, eccentric wall thickening in the ileocaecal region (arrows) without narrowing of the lumen (*) and with the impression on ultrasound of preservation of the layered structure, despite the extent of the thickening. This is accompanied by a cluster of enlarged mesenteric lymph nodes (arrowheads), which is more precisely defined on ultrasound, as well as numerous focal liver lesions (discontinuous arrows) and ascites (+). The patient remains in complete remission four years after starting chemotherapy. G) High-grade mantle-cell lymphoma involving the splenic flexure of the colon. 69-year-old female. Left image: coronal CT. Right image: ultrasound. Large mass encompassing the splenic flexure of the colon (c) and extending towards the mesocolon (arrows). Accompanied by involvement of the distal ileum (i), gallbladder (g) and uterus (u) in the form of visceral thickening, as well as mesenteric lymphadenopathy (arrowheads), ascites (+) and peritoneal lymphomatosis (discontinuous arrows). The diagnosis was obtained with ultrasound-guided percutaneous biopsy of the mesocolon mass (empty arrows).

carcinoids of the distal ileum, where they are also the most common type of neoplasm. They are small (15—35 mm) submucosal tumours, hypoechoic or with an echogenic halo.[35,37,56] The secretion of serotonin means they can cause obstruction due to retraction of the bowel. Endometriosis can mimic them.[35] They tend to spread to the mesentery as mild lymphadenopathy or in the form of hypoechoic desmoplastic masses, often with calcifications, which can be the dominant finding and cause mesenteric and tributary bowel congestion.[35,36,55,56] Ultrasound detects 13–76.5% of primary tumours (26–40% multiple).[55,56] Both these and lymph node or liver metastases show intense and early enhancement, sometimes peripherally.[35,58] The intensity and the pattern

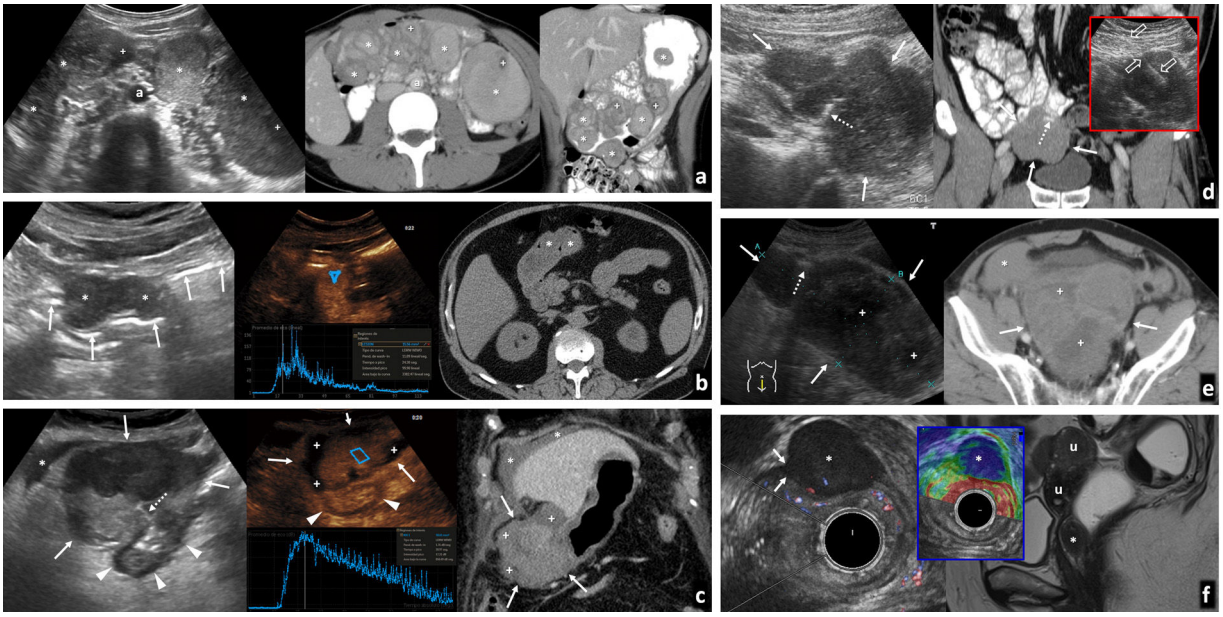

**Figure 8** Gastrointestinal stromal tumours (GIST). A) Multiple gastric GIST in the context of Carney-Stratakis syndrome. There are also several neck paragangliomas (not shown). 20-year-old female. From left to right: ultrasound (transverse section in epigastrium), axial computed tomography (CT) with oral and intravenous contrast in the same plane, and coronal CT. There are innumerable solid nodules and masses (*) of various echogenicities attached to the stomach wall. In some there are cystic or necrotic degeneration foci (+). a: aorta. There was no response to imatinib and the patient required subtotal gastrectomy. There was no mutation in c-KIT or PDGFRA and there was a germline mutation in an SDH subunit (common in these cases). GIST in syndromes affect more young women and girls, with a histological subtype more frequently epithelioid than spindle cell. They commonly appear as multiple gastric tumours, lymphadenopathy is not so unusual and they are much less likely to respond to imatinib than sporadic tumours. B) Small stomach GIST with endophytic growth. 71-year-old male. From left to right: ultrasound (transverse section in epigastrium), ultrasound with contrast and axial CT without contrast (history of severe adverse reaction). Incidental ultrasound finding of a homogeneously hypoechoic lobulated tumour (*) with endophytic growth in the antrum of the stomach. Despite this being a study with a low frequency convex probe in an obese patient, we are able to see that the lesion is attached to the muscularis propria and is immediately superficial to the more proximal echogenic submucosa layer. The arrows indicate the gastric lumen. In contrast-enhanced ultrasound, the lesion enhances quickly and homogeneously, with subsequent washout. Certain machines and PACS (picture archiving and communications systems) make quantitative analysis possible. In CT without contrast, the lesion goes practically unnoticed. C) Stomach GIST with exophytic growth and spontaneous haemorrhagic complication. 82-year-old female. Abdominal pain and anaemia. From left to right: ultrasound (cross section in the right hypochondriac region), contrast-enhanced ultrasound, and contrast-enhanced coronal CT. Heterogeneous mass (arrows) with exophytic growth from the antrum of the stomach (arrowheads) and an ulceration (dashed arrow). Peritoneal fluid (*) with fine echoes and dense on baseline CT (not shown). Contrast-enhanced ultrasound shows intense and rapid enhancement, with delayed washout. At the periphery of the mass there is no enhancement (+). On CT it corresponds to a sentinel clot. In surgery, haemoperitoneum was found and a bleeding GIST resected in the stomach. D) Ulcerated ileal GIST with exophytic growth. 66-year-old male with melaena. Left image: ultrasound. Right image: coronal CT scan with oral and intravenous contrast. Inset: ultrasound-guided biopsy (empty arrows). Lobulated mass of intermediate echogenicity growing exophytically from the proximal ileum (arrows), with mucosal ulceration (discontinuous arrows). E) Haemorrhagic GIST of the colon. 72-year-old male. Left image: ultrasound (longitudinal section in the hypogastrium). Right image: axial CT with contrast. Large heterogeneous mass (arrows), with large necrotic areas (+), an intralesional gas bubble due to cavitation (dashed arrow) and haemoperitoneum (*). Attached to the distal sigmoid colon. F) Small rectal GIST. Left image: transrectal Doppler ultrasound. Right image: T2-weighted sagittal magnetic resonance imaging with endorectal gel. Central inset: strain elastography. Homogeneously hypoechoic nodular lesion in the anterior aspect of the lower rectum (*), with high tissue stiffness in qualitative elastography. Ultrasound shows its attachment to the hypoechoic muscularis propria (arrows). u: myomatous uterus.

of enhancement and washout have been correlated with tumour grade.[58]

They are very uncommon in the duodenum and proximal jejunum. Carcinoids or gastrinomas can also occur[55,59] with typical lymphadenopathy and less desmoplastic behaviour. NET account for 1% of gastric neoplasms. Type I (70–80%) are secondary to chronic atrophic gastritis, and are non-invasive and small. Type II (5–6%) are gastrinomas, also non-invasive and small, and can cause Zollinger-Ellison syndrome. Type III (15–20%) are invasive and aggressive, mimicking adenocarcinoma.[55,56]

The rectum is the second most common site for gastrointestinal NET. They are small and localized, and have a good prognosis.[56] On TRUS they appear hypoechoic, confined to the submucosa.

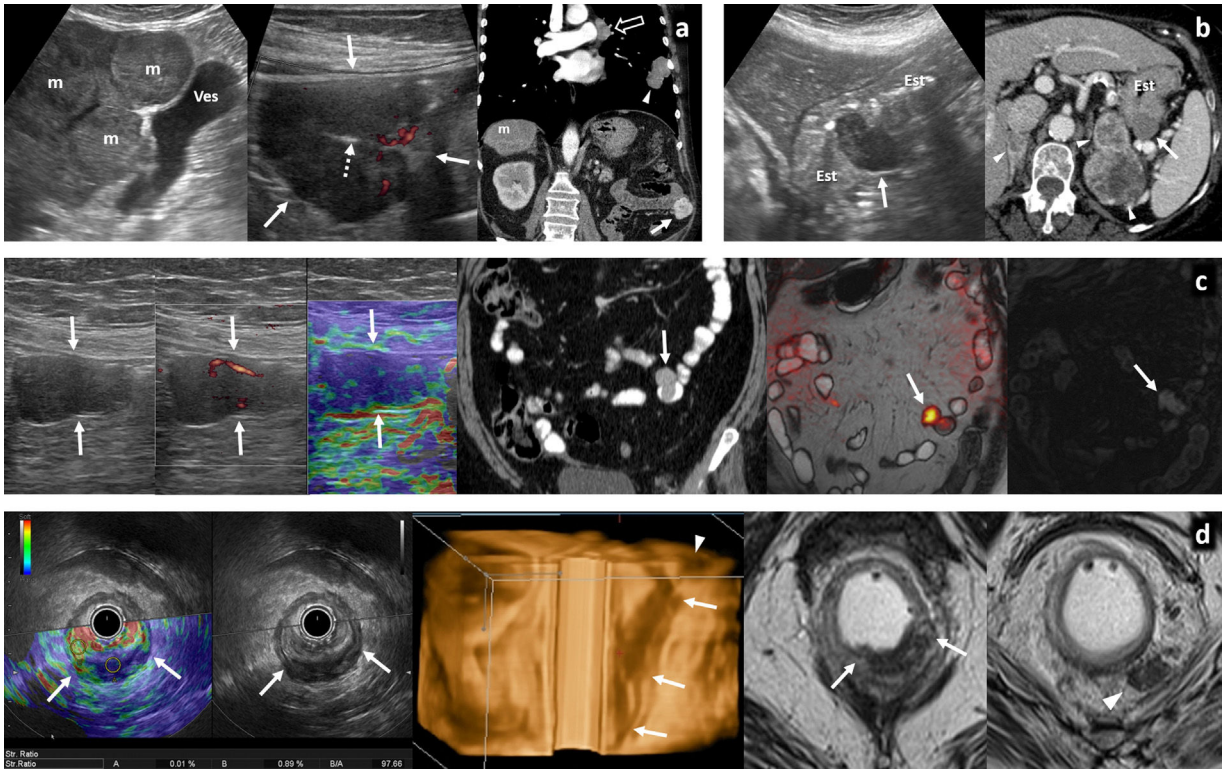


**Figure 9** Bowel metastasis. A) Ulcerated jejunal metastasis of a pulmonary neuroendocrine tumour. 65-year-old male. Constitutional syndrome. From left to right: liver ultrasound, left flank ultrasound, and coronal contrast-enhanced computed tomography (CT). Primary lung tumour (arrowhead), mediastinal lymphadenopathy (empty arrow), liver metastases (m), and hypoechoic and hypervascular jejunal metastases (arrows), with ulceration (broken arrow). B) Gastric metastasis of clear-cell renal cell carcinoma. 72-year-old female. Left image: longitudinal ultrasound in epigastrium. Right image: axial CT with contrast. Hypoechoic lobulated metastasis (arrows) in the posterior wall of the body of the stomach (St). There are also adrenal (arrowheads), cardiac, peritoneal, bone and soft tissue metastases (not shown). C) Endo- and exophytic jejunal metastasis of acral lentiginous melanoma. 56-year-old female. From left to right: left flank ultrasound, Doppler ultrasound, strain elastography, coronal CT with oral and intravenous contrast, coronal fusion/diffusion T2-weighted magnetic resonance (MR) enterography, coronal T1-weighted image without contrast. Lobulated metastasis, with an endophytic and an exophytic component in a stretch of jejunum (arrows). It is hypoechoic, moderately vascularised, stiff on elastography, homogeneous on CT, with diffusion restriction and moderately hyperintense on T1-weighted images due to melanin content. D) Anorectal melanoma. 64-year-old female. From left to right: strain elastography and transrectal ultrasound in lower rectum, 3 D reconstruction of endorectal ultrasound, axial T2-weighted magnetic resonance imaging (MRI) in a lower and upper plane. Infiltrating lesion in the posterior wall of the lower rectum and anus with great tissue stiffness (strain ratio of 97.66), embedded in the submucosa with mucosal and transmural infiltration (arrows), as well as peri-rectal lymphadenopathy (arrowheads). There was also invasion of extramural veins and liver metastases (not shown). No cutaneous melanoma was found.

With the exception of appendiceal NET, in the colon NET are very rare and aggressive. In the appendix (where 60% of tumours are NET; an incidental finding in appendectomy specimens in 70% of cases[56]), the prognosis is generally good.

## Haematological tumours (Fig. 7)

Although rare (1–8%), the gastrointestinal tract is the most common extranodal site of lymphoma, almost always primary or secondary non-Hodgkin's B-cell lymphoma. The stomach is the most commonly involved site, followed by the small bowel (especially distal ileum), colon-rectum and oesophagus. On ultrasound, lymphoma can appear as a mass or, more likely, marked hypoechoic circumferential wall thickening, more homogeneous, longer and less obstructive than carcinoma, with the layer structure often comparatively preserved. It can be multifocal and cause ulceration and cavitation and, due to destruction of the myenteric plexus, lead to aneurysmal lumen dilation. It is often accompanied by prominent hypoechoic lymphadenopathy, and sometimes involvement of the peritoneum or other organs. With contrast, it shows homogeneous enhancement, milder and more delayed than other tumours[36,59,60] Fig. 7.

The most common subtype is *diffuse large-cell lymphoma* (40–78%), which is aggressive and high-grade. The second most common is *extranodal marginal zone lymphoma* (formerly MALT lymphoma), which is lower grade and includes immunoproliferative small intestinal disease or Mediterranean lymphoma. They are followed by *mantle-cell* (5–13%, aggressive), *follicular* (5–12%, with good prognosis), *Burkitt* (5%, aggressive, more common in children and immunosuppressed, generally as an ileocaecal mass), *T-cell associated with enteropathy* (3–4%, in treatment-

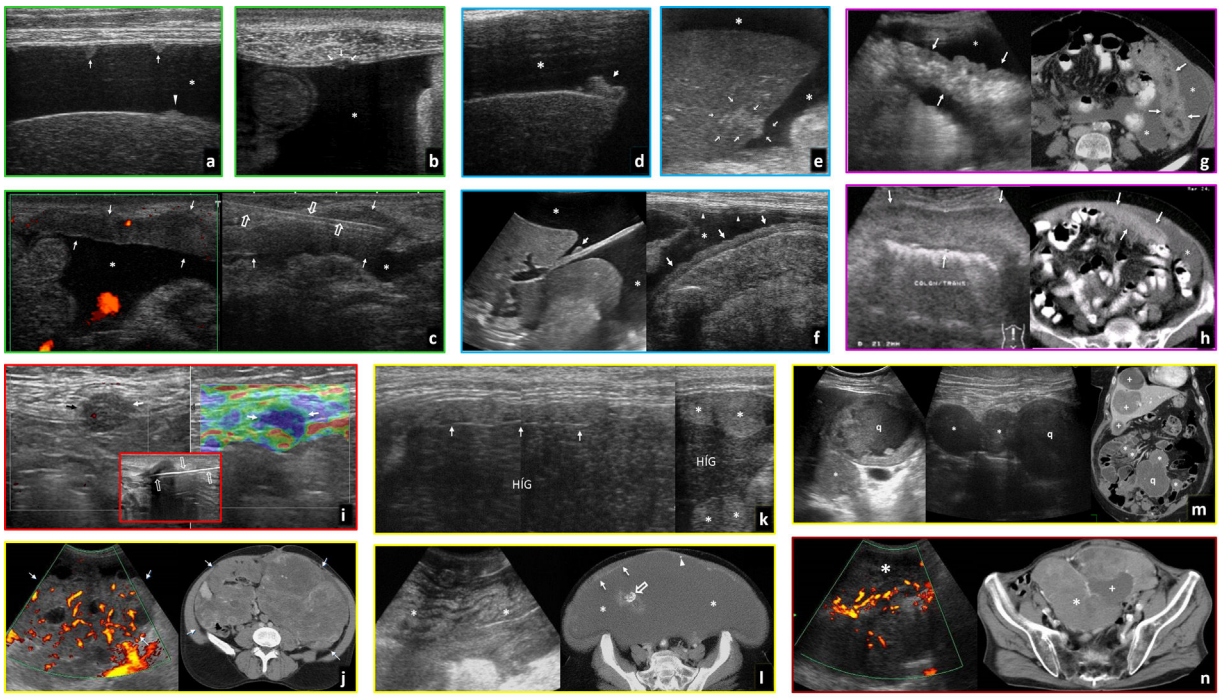


**Figure 10** Peritoneal and subperitoneal neoplasms. Green box: parietal peritoneum. Blue box: visceral peritoneum. Purple box: greater omentum. Red box: invasion of wall. Yellow box: other types of cancer. Brown box: subperitoneal mesenchymal tumours. A) Ovarian cancer. Very small implants in the parietal peritoneum (arrows) in the presence of ascites (*). Small implant in the hepatic visceral peritoneum (arrowhead). B) Stomach cancer. Very small peritoneal implant (arrows) invading the *fascia transversalis* and the right anterior rectus muscle of the abdomen (there is no deep muscle fascia below the arcuate line) in the presence of ascites (*). C) Ovarian cancer. Linear thickening of the parietal peritoneum (arrows) and ascites (*). Ultrasound helps guide the biopsy of the smooth thickening of the peritoneum (empty arrows). D) Bladder cancer. Nodular implant in the hepatic visceral peritoneum, without parenchymal invasion (arrow) and ascites (*). E) Ovarian cancer. Nodular implant in the hepatic visceral peritoneum, with parenchymal invasion (arrow) and ascites (*). F) Endometrial cancer. Left image: millimetric nodular implant in the visceral peritoneum covering the extrahepatic falciform ligament (arrow). Ascitis (*). Right image: smooth thickening of the visceral peritoneum on a stretch of small bowel (arrows) and ascites (*). Smooth thickening of the parietal peritoneum (arrowheads). G) Colon cancer. Striated infiltration of the omentum (omental "smudging"). Thickening of the visceral peritoneum of the greater omentum and fat stranding (hypoechoic and hyperdense, respectively, in relation to the fat) (arrows) and ascites (*). H) Ovarian cancer. Diffuse infiltration of the omentum (omental "cake"). Diffuse infiltration of the gastrocolic ligament and its continuation below the transverse colon (greater omentum) (arrows) and ascites (*). I) Colon cancer. Implant in parietal peritoneum with direct invasion of the wall (arrows), with ultrasound and qualitative elastography, without ascites. In the inset, percutaneous biopsy in another similar case (empty arrows). J) Peritoneal desmoplastic small round cell tumour. Large omental, mesenteric and peritoneal masses (arrows) with abundant vascularisation in a young male. K) Mucinous peritoneal carcinomatosis due to gastric adenocarcinoma. Perihepatic echoic covering layer (arrows) and echoic mucinous implants (*) with scalloping of the liver (LIV). L) Peritoneal adenomucinosis. Massive inframesocolic occupation by complex mucinous material (*), with alternating echogenicities and converging into a central calcification (empty arrow). The complexity of the mucinous material is reflected much better on ultrasound than computed tomography (CT). Implants with fine calcifications (arrowheads) in a thickened parietal peritoneum (arrows). M) GIST with peritoneal and hepatic spread. Numerous rounded nodular lesions in both the liver (+) and the peritoneal cavity (*), the largest with cystic and/or necrohaemorrhagic changes (q). N) GIST of sigmoid mesocolon. Doppler ultrasound and CT. Large hypervascular pelvic mass (*) with cystic or necrotic areas (+).

resistant coeliac disease, proximal, with poor prognosis) and *post-transplant* (especially renal). Other haematological neoplasms can affect the intestine and mesentery: *multiple myeloma and plasmacytoma* (wall thickening or mass), *mastocytosis* (wall thickening, hepatosplenomegaly, lymphadenopathy and sclerosing bone lesions), *myeloid or granulocytic sarcoma or chloroma* (in acute myeloid leukaemia or others, as a mass or wall thickening) and *Castleman's disease* (polyclonal lymphoproliferative disorder with mesenteric lymphadenopathy).[60,61]

## GIST and other mesenchymal tumours (Fig. 8)

GIST, derived from the interstitial cells of Cajal, are by far the most common gastrointestinal mesenchymal neoplasm, generally forming in the muscle layer. Approximately 60% affect the stomach, 30% the small bowel and 4% colon-rectum. The mean age at diagnosis is 60, lower in syndromes (Carney-Stratakis syndrome, Carney's triad, type 1 neurofibromatosis) in which the ALARA principles (''As Low As Reasonably Achievable'') are particularly relevant[62] Fig. 8.

They are delimited, rounded or lobulated hypoechoic tumours, generally with non-infiltrating exophytic growth, commonly with areas of cystic, haemorrhagic or necrotic (hypo-anechoic) degeneration when large. They may have calcifications, ulcerate and bleed into the intestine or peritoneum. They tend to metastasise to the peritoneum (also as round tumours) and the liver, with lymphadenopathy rare. Various prognostic staging systems consider radiological aspects (size, heterogeneity, ulceration, location, intensity and enhancement pattern) and non-radiological aspects (mitotic index, histological subtype, differentiation, pleomorphism, surgical rupture).[35,36,63,64]

Solid areas are intensely enhanced with ultrasound contrast, which also helps guide biopsies and shows potential as a prognostic marker and in the follow-up of patients treated with imatinib.[64,65] The intense and heterogeneous enhancement also allows them to be differentiated from leiomyoma (much more common in the oesophagus) and other benign mesenchymal tumours, which may be morphologically similar, but tend to enhance less, and homogeneously.[35,65–67] It is less certain whether GIST are significantly stiffer than leiomyomas on endoscopic ultrasound elastography.[66,68] Lipomas tend to be hyperechoic.[29] Malignant mesenchymal tumours are not distinguishable from GIST by imaging.

## Metastasis

The most common origins are melanoma, lung cancer and renal cell carcinoma.[29,59] The existence of primary intestinal melanoma is debatable.[69] Metastases behave like hypoechoic submucosal nodules, sometimes multiple, and occasionally with circumferential infiltration, endoluminal growth or ulceration. Knowing the oncological history is key Fig. 9.

## Peritoneal and subperitoneal tumours (Figs. 10 and 11, video 3)

Ultrasound is the ideal technique for detecting ascites and defining it as exudative (with echoes, septa and loculations). Although it requires experience and dedication, it is also extremely useful in the study of *carcinomatosis* and other forms of peritoneal neoplastic involvement, as it can detect even millimetric peritoneal implants and in the absence of ascites, more or less nodular thickening of the peritoneal surfaces and infiltration of the greater omentum, very accessible due to its anatomical situation, whether attached or not to the parietal peritoneum.[32,33] Contrast is more sensitive than Doppler in demonstrating vascularisation in affected areas. In the omentum, contrast enhances both the echogenic areas and the hypoechoic nodules, with the nodules showing radial filling and faster washout. It is useful for differentiating from tuberculosis (with less enhancement) and choosing where to biopsy.[70,71] Fig. 10

The findings in *mesothelioma* and *primary serous carcinoma*, as well as in peritoneal *lymphomatosis*, are similar with nuances. *Desmoplastic small round cell tumours* have a poor prognosis and affect young men in the form of one or multiple heterogeneous solid masses, with or without ascites.[33]

In *Pseudomyxoma peritonei*, the peritoneal cavity fills up with mucinous material, almost always due to a ruptured appendiceal mucocele. On ultrasound, it appears like a space-occupying lesion with diverse echogenicities, occasionally alternating, with calcifications, nodules or echogenic peritoneal covering layer and visceral scalloping.

Many different *mesenchymal neoplasms* can affect the mesentery or omentum, behaving as solid masses and with malignant variants tending to be larger and more heterogeneous and infiltrating.[33]

## Ultrasound as a guide to percutaneous biopsy (video 4)

This can be required in lesions of almost any type and origin when the endoscopic approach fails or is not possible, with a multidisciplinary decision on the benefit-risk ratio. Ultrasound guidance is cheaper, more versatile, safer, faster and more effective than CT guidance. Gradual compression displaces the intestine, brings the lesions closer and holds them in place. Core needle biopsy is more cost-effective. With 18F needles it is safe to go through (better transversely) the wall of the stomach or small bowel, but not the colon. It is successful in more than 90%, with low complication rates,[72–74] including in children.[75]

## Authorship

1 Person responsible for the integrity of the study: MÁCC.
2 Study conception: MÁCC and JEI.
3 Study design: MÁCC and JEI.
4 Data acquisition: MÁCC and JEI.
5 Data analysis and interpretation: MÁCC and JEI.
6 Statistical processing: not applicable.
7 Literature search: MÁCC and JEI.
8 Drafting of the article: MÁCC and JEI.
9 Critical review of the manuscript with relevant intellectual contributions: MÁCC and JEI.
10 Approval of the final version: MÁCC and JEI.

## Conflicts of interest

The authors declare that they have no conflicts of interest.

## Appendix A. Supplementary data

Supplementary material related to this article can be found, in the online version, at doi:https://doi.org/10.1016/j.rx.2020.12.004.

## References

1. Roccarina D, Garcovich M, Ainora ME, Caracciolo G, Ponziani F, Gasbarrini A, et al. Diagnosis of bowel diseases: the role of imaging and ultrasonography. World J Gastroenterol. 2013;19:2144–53, http://dx.doi.org/10.3748/wjg.v19.i14.2144.
2. Medellin A, Merrill C, Wilson SR. Role of contrast-enhanced ultrasound in evaluation of the bowel.

Abdom Radiol (NY). 2018;43:918–33, http://dx.doi.org/10.1007/s00261-017-1399-6.
3. Transabdominal ultrasonography of the small and large intestine. In: Saltzman JR, Robson KM, eds. Uptodate. https://www.uptodate.com.
4. Mazzie JP, Wilson SR, Sadler MA, Khalili M, Javors BR, Weston SR, et al. Imaging of gastrointestinal tract infection. Semin Roentgenol. 2007;42:102–16, http://dx.doi.org/10.1053/j.ro.2006.08.013.
5. Lalchandani UR, Weadock WJ, Brady GF, Wasnik AP. Imaging in gastric anisakiasis. Clin Imaging. 2018;50:286–8, http://dx.doi.org/10.1016/j.clinimag.2018.04.018.
6. Shibata E, Ueda T, Akaike G, Saida Y. CT findings of gastric and intestinal anisakiasis. Abdom Imaging. 2014;39:257–61, http://dx.doi.org/10.1007/s00261-014-0075-3.
7. Shimamura Y, Muwanwella N, Chandran S, Kandel G, Marcon N. Common symptoms from an uncommon infection: gastrointestinal anisakiasis. Can J Gastroenterol Hepatol. 2016;2016:5176502, http://dx.doi.org/10.1155/2016/5176502.
8. Kanar O, Nakshabendi R, Jiwani F, Liu Y, Allsopp W, Berry AC. Giardiasis: a malignant mimicker? Intern Emerg Med. 2016;11:149–51, http://dx.doi.org/10.1007/s11739-015-1267-8.
9. Duffin C, Mirpour S, Catanzano T, Moore C. Radiologic imaging of bowel infections. Semin Ultrasound CT MR. 2020;41:33–45, http://dx.doi.org/10.1053/j.sult.2019.10.004.
10. Kothary NN, Muskie JM, Mathur SC. Strongyloides stercoralis hyperinfection. Radiographics. 1999;19:1077–81, http://dx.doi.org/10.1148/radiographics.19.4.g99jl171077.
11. Nalaboff KM, Rozenshtein A, Kaplan MH. Imaging of mycobacterium avium-intracellulare infection in AIDS patients on highly active antiretroviral therapy: reversal syndrome. AJR Am J Roentgenol. 2000;175:387–90, http://dx.doi.org/10.2214/ajr.175.2.1750387.
12. Puylaert JB, Van der Zant FM, Mutsaers JA. Infectious ileocecitis caused by Yersinia, Campylobacter, and Salmonella: clinical, radiological and US findings. Eur Radiol. 1997;7:3–9, http://dx.doi.org/10.1007/s003300050098.
13. Hennedige T, Bindl DS, Bhasin A, Venkatesh SK. Spectrum of imaging findings in Salmonella infections. AJR Am J Roentgenol. 2012;198:W534–9, http://dx.doi.org/10.2214/AJR.11.7621.
14. Rees JH, Soudain SE, Gregson NA, Hughes RA. Campylobacter jejuni infection and Guillain-Barré syndrome. N Engl J Med. 1995;333:1374–9, http://dx.doi.org/10.1056/NEJM199511233332102.
15. Deshpande SS, Joshi AR, Deshpande SS, Phajlani SA. Computed tomographic features of abdominal tuberculosis: unmask the impersonator! AbdomRadiol (NY). 2019;44:11–21, http://dx.doi.org/10.1007/s00261-018-1700-3.
16. Malik A, Saxena NC. Ultrasound in abdominal tuberculosis. Abdom Imaging. 2003;28:574–9, http://dx.doi.org/10.1007/s00261-002-0061-z.
17. Raut AA, Naphade PS, Ramakantan R. Imaging spectrum of extrathoracic tuberculosis. Radiol Clin North Am. 2016;54:475–501, http://dx.doi.org/10.1016/j.rcl.2015.12.013.
18. Gupta P, Kumar S, Sharma V, Mandavdhare H, Dhaka N, Sinha SK, et al. Common and uncommon imaging features of abdominal tuberculosis. J Med Imaging Radiat Oncol. 2019;63:329–39, http://dx.doi.org/10.1111/1754-9485.12874.
19. Pereira JM, Madureira AJ, Vieira A, Ramos I. Abdominal tuberculosis: imaging features. Eur J Radiol. 2005;55:173–80, http://dx.doi.org/10.1016/j.ejrad.2005.04.015.
20. Almalki M, Yaseen W. Cecal ameboma mimicking obstructing colonic carcinoma. J Surg Case Rep. 2018;2018:rjy124, http://dx.doi.org/10.1093/jscr/rjy124.
21. Tsujimoto T, Kuriyama S, Yoshiji H, Fujimoto M, Kojima H, Yoshikawa M, et al. Ultrasonographic findings of amebic colitis. J Gastroenterol. 2003;38:82–6, http://dx.doi.org/10.1007/s005350300011.
22. Frickenstein AN, Jones MA, Behkam B, McNally LR. Imaging Inflammation and Infection in the Gastrointestinal Tract. Int J Mol Sci. 2019;21:E243, http://dx.doi.org/10.3390/ijms21010243.
23. Butler T. Haemolytic uraemic syndrome during shigellosis. Trans R Soc Trop Med Hyg. 2012;106:395–9, http://dx.doi.org/10.1016/j.trstmh.2012.04.001.
24. Lamb CA, Lamb EI, Mansfield JC, Sankar KN. Sexually transmitted infections manifesting as proctitis. Frontline Gastroenterol. 2013;4:32–40, http://dx.doi.org/10.1136/flgastro-2012-100274.
25. Ramachandran I, Sinha R, Rodgers P. Pseudomembranous colitis revisited: spectrum of imaging findings. Clin Radiol. 2006;61:535–44, http://dx.doi.org/10.1016/j.crad.2006.03.009.
26. Shieh AC, Guler E, Tirumani SH, Dumot J, Ramaiya NH. Clinical, imaging, endoscopic findings and management of patients with CMV colitis: a single-institute experience. Emerg Radiol. 2020;27:277–84, http://dx.doi.org/10.1007/s10140-020-01750-z.
27. Miller FH, Ma JJ, Scholz FJ. Imaging features of enterohemorrhagic Escherichia coli colitis. AJR Am J Roentgenol. 2001;177:619–23, http://dx.doi.org/10.2214/ajr.177.3.1770619.
28. Wale A, Pilcher J. Current role of ultrasound in small bowel imaging. Semin Ultrasound CT MR. 2016;37:301–12, http://dx.doi.org/10.1053/j.sult.2016.03.001.
29. Cavalcoli F, Zilli A, Fraquelli M, Conte D, Massironi S. Small bowel ultrasound beyond inflammatory bowel disease: an updated review of the recent literature. Ultrasound Med Biol. 2017;43:1741–52, http://dx.doi.org/10.1016/j.ultrasmedbio.2017.04.028.
30. Childers BC, Cater SW, Horton KM, Fishman EK, Johnson PT. CT evaluation of acute enteritis and colitis: is it infectious, inflammatory, or ischemic?: Resident and fellow education feature. Radiographics. 2015;35:1940–1, http://dx.doi.org/10.1148/rg.2015150125.
31. García A, Rodríguez P, Méndez R. Infección intestinal. Afectación difusa del tubo digestivo. In: Del Cura JL, Pedraza S, Gayete A, Rovira A, editors. Radiología Esencial. SERAM. 2.ª ed. Madrid: Médica Panamericana; 2018. p. 682–95.
32. Hanbidge AE, Lynch D, Wilson SR. US of the peritoneum. Radiographics. 2003;23:663–85, http://dx.doi.org/10.1148/rg.233025712.
33. Corral MA, Girela E, Encinas J. Patología del peritoneo, del mesenterio y de la pared abdominal. In: Del Cura JL, Pedraza S, Gayete A, Rovira A, editors. Radiología Esencial. SERAM. 2.ª ed Madrid: Médica Panamericana; 2018. p. 796–810.
34. Expert Panel on Gastrointestinal Imaging, Fowler KJ, Kaur H, Cash BD, Feig BW, Gage KL, et al. ACR Appropriateness Criteria (®) Pretreatment Staging of Colorectal Cancer. Am Coll Radiol. 2017;14:S234–44, http://dx.doi.org/10.1016/j.jacr.2017.02.012.
35. Nylund K, Maconi G, Hollerweger A, Ripolles T, Pallotta N, Higginson A, et al. EFSUMB recommendations and guidelines for gastrointestinal ultrasound. Ultraschall Med. 2017;38:e1–15, http://dx.doi.org/10.1055/s-0042-115853.
[36]. Muradali D, Goldberg DR. US of gastrointestinal tract disease. Radiographics. 2015;35:50–68, http://dx.doi.org/10.1148/rg.351140003.
37. Kralik R, Trnovsky P, Kopálová M. Transabdominal ultrasonography of the small bowel. Gastroenterol Res Pract. 2013:24348544, http://dx.doi.org/10.1155/2013/896704.

38. Encinas de la Iglesia J, Corral de la Calle MA, Fernández Pérez GC, Ruano Pérez R, Álvarez Delgado A. Cáncer de esófago: particularidades anatómicas, estadificación y técnicas de imagen. Radiologia. 2016;58:352–65, http://dx.doi.org/10.1016/j.rx.2016.06.004.
39. Cârțână ET, Gheonea DI, Săftoiu A. Advances in endoscopic ultrasound imaging of colorectal diseases. World J Gastroenterol. 2016;22:1756–66, http://dx.doi.org/10.3748/wjg.v22.i5.1756.
40. Hasak S, Kushnir V. Rectal endoscopic ultrasound in clinical practice. Curr Gastroenterol Rep. 2019;21:18, http://dx.doi.org/10.1007/s11894-019-0682-9.
41. Pickhardt PJ, Pooler BD, Kim DH, Hassan C, Matkowskyj KA, Halberg RB. The natural history of colorectal polyps: overview of predictive static and dynamic features. Gastroenterol Clin North Am. 2018;47:515–36, http://dx.doi.org/10.1016/j.gtc.2018.04.004.
42. Koichi Y, Shigeru S, Hiroya F, Shinji T, Masayuki F. Transabdominal sonographic appearance of adult colonic polyps. J Med Ultrason. 2006;33:231–7, http://dx.doi.org/10.1007/s10396-006-0112-0.
43. Limberg B. Diagnosis and staging of colonic tumors by conventional sonography as compared with hydrocolonic sonography. N Engl J Med. 1992;327:65–9, http://dx.doi.org/10.1056/NEJM199207093270201.
44. Hosokawa T, Hosokawa M, Tanami Y, Sato Y, Nambu R, Iwama I, et al. Diagnostic performance of ultrasound without any colon preparation for detecting colorectal polyps in pediatric patients. Pediatr Radiol. 2019;49:1306–12, http://dx.doi.org/10.1007/s00247-019-04467-5.
45. Qu NN, Liu RH, Shi L, Cao XL, Yang YJ, Li J. Sonographic diagnosis of colorectal polyps in children: Diagnostic accuracy and multi-factor combination evaluation. Medicine (Baltimore). 2018;97:e12562, http://dx.doi.org/10.1097/MD.0000000000012562.
46. Li T, Lu M, Song J, Wu P, Cheng X, Zhang Z. Improvement to ultrasonographical differential diagnosis of gastric lesions: the value of contrast enhanced sonography with gastric distention. PLoS One. 2017;12:e0182332, http://dx.doi.org/10.1371/journal.pone.0182332.
47. hi H, Yu XH, Guo XZ, Guo Y, Zhang H, Qian B, et al. Double contrast-enhanced two-dimensional and three-dimensional ultrasonography for evaluation of gastric lesions. World J Gastroenterol. 2012;18:4136–44, http://dx.doi.org/10.3748/wjg.v18.i31.4136.
48. Kuzmich S, Harvey CJ, Kuzmich T, Tan KL. Ultrasound detection of colonic polyps: perspective. Br J Radiol. 2012;85:e1155–64, http://dx.doi.org/10.1259/bjr/60593124.
49. Greif F, Aranovich D, Zilbermints V, Hannanel N, Belenky A. Intraoperative hydrocolonic ultrasonography for localization of small colorectal tumors in laparoscopic surgery. Surg Endosc. 2010;24:3144–8, http://dx.doi.org/10.1007/s00464-010-1106-y.
50. Greif F, Belenky A, Aranovich D, Yampolski I, Hannanel N. Intraoperative ultrasonography: a tool for localizing small colonic polyps. Int J Colorectal Dis. 2005;20:502–6, http://dx.doi.org/10.1007/s00384-004-0716-z.
51. Martínez-Ares D, Martín-Granizo Barrenechea I, Souto-Ruzo J, Yáñez López J, Pallarés Peral A, Vázquez-Iglesias JL. The value of abdominal ultrasound in the diagnosis of colon cancer. Rev Esp Enferm Dig. 2005;97:877–86, http://dx.doi.org/10.4321/s1130-01082005001200004.
52. Shibasaki S, Takahashi N, Homma S, Nishida M, Shimokuni T, Yoshida T, et al. Use of transabdominal ultrasonography to preoperatively determine T-stage of proven colon cancers. Abdom Imaging. 2015;40:1441–50, http://dx.doi.org/10.1007/s00261-014-0296-5.
53. Chung HW, Chung JB, Park SW, Song SY, Kang JK, Park CI. Comparison of hydrocolonic sonography accuracy in preoperative staging between colon and rectal cancer. World J Gastroenterol. 2004;10:1157–61, http://dx.doi.org/10.3748/wjg.v10.i8.1157.
54. Leshchinskiy S, Ali N, Akselrod D. The onion skin sign of appendiceal mucocele. Abdom Radiol (NY). 2018;43:2527–8, http://dx.doi.org/10.1007/s00261-018-1489-0.
55. Basuroy R, Srirajaskanthan R, Ramage JK. Neuroendocrine tumors. Gastroenterol Clin North Am. 2016;45:487–507, http://dx.doi.org/10.1016/j.gtc.2016.04.007.
56. Sahani DV, Bonaffini PA, Fernández-Del Castillo C, Blake MA. Gastroenteropancreatic neuroendocrine tumors: role of imaging in diagnosis and management. Radiology. 2013;266:38–61, http://dx.doi.org/10.1148/radiol.12112512.
57. Sanli Y, Garg I, Kandathil A, Kendi T, Zanetti MJB, Kuyumcu S, et al. Neuroendocrine Tumor Diagnosis and Management: (68)Ga-DOTATATE PET/CT. AJR Am J Roentgenol. 2018;211:267–77, http://dx.doi.org/10.2214/AJR.18.19881.
58. Dörffel Y, Wermke W. Neuroendocrine tumors: characterization with contrast-enhanced ultrasonography. Ultraschall Med. 2008;29:506–14, http://dx.doi.org/10.1055/s-2008-1027555.
59. Barat M, Dohan A, Dautry R, Barral M, Boudiaf M, Hoeffel C, et al. Mass-forming lesions of the duodenum: a pictorial review. Diagn Interv Imaging. 2017;98:663–75, http://dx.doi.org/10.1016/j.diii.2017.01.004.
60. Hanafy AK, Morani AC, Menias CO, Pickhardt PJ, Shaaban AM, Mujtaba B, et al. Hematologic malignancies of the gastrointestinal luminal tract. Abdom Radiol (NY). 2019, http://dx.doi.org/10.1007/s00261-019-02278-8.
61. Brodzisz A, Woźniak MM, Dudkiewicz E, Grabowski D, Stefaniak J, Wieczorek AP, et al. Ultrasound presentation of abdominal non-Hodgkin lymphomas in pediatric patients. J Ultrason. 2013;13:373–8, http://dx.doi.org/10.15557/JoU.2013.0040.
62. Herzberg M, Beer M, Anupindi S, Vollert K, Kröncke T. Imaging pediatric gastrointestinal stromal tumor (GIST). J Pediatr Surg. 2018;53:1862–70, http://dx.doi.org/10.1016/j.jpedsurg.2018.03.022.
63. Scola D, Bahoura L, Copelan A, Shirkhoda A, Sokhandon F. Getting the GIST: a pictorial review of the various patterns of presentation of gastrointestinal stromal tumors on imaging. Abdom Radiol (NY). 2017;42:1350–64, http://dx.doi.org/10.1007/s00261-016-1025-z.
64. Danti G, Addeo G, Cozzi D, Maggialetti N, Lanzetta MM, Frezzetti G, et al. Relationship between diagnostic imaging features and prognostic outcomes in gastrointestinal stromal tumors (GIST). Acta Biomed. 2019;90:9–19, http://dx.doi.org/10.23750/abm.v90i5-S.8343.
65. Alvarez-Sanchez MV, Gincul R, Lefort C, Napoleon B. Role of contrast-enhanced harmonic endoscopic ultrasound in submucosal tumors. Endosc Ultrasound. 2016;5:363–7, http://dx.doi.org/10.4103/2303-9027.190928.
66. Ignee A, Jenssen C, Hocke M, Dong Y, Wang WP, Cui XW, et al. Contrast-enhanced (endoscopic) ultrasound and endoscopic ultrasound elastography in gastrointestinal stromal tumors. Endosc Ultrasound. 2017;6:55–60, http://dx.doi.org/10.4103/2303-9027.200216.
67. Kamata K, Takenaka M, Kitano M, Omoto S, Miyata T, Minaga K, et al. Contrast-enhanced harmonic endoscopic ultrasonography for differential diagnosis of submucosal tumors of the upper gastrointestinal tract. J Gastroenterol Hepatol. 2017;32:1686–92, http://dx.doi.org/10.1111/jgh.13766.
68. Tsuji Y, Kusano C, Gotoda T, Itokawa F, Fukuzawa M, Sofuni A, et al. Diagnostic potential of endoscopic ultrasonography-elastography for gastric submucosal tumors: a pilot study. Dig Endosc. 2016;28:173–8, http://dx.doi.org/10.1111/den.12569.
69. Benaissa A, Fornès P, Ladam-Marcus V, Grange F, Amzallag-Bellenger E, Hoeffel C. Multimodality imag-

ing of melanoma metastases to the abdomen and pelvis. Clin Imaging. 2011;35:452–8, http://dx.doi.org/10.1016/j.clinimag.2011.01.013.
70. Que Y, Wang X, Tao C, Zhang Y, Wan W, Chen B. Peritoneal metastases: evaluation with contrast-enhanced ultrasound. Abdom Imaging. 2011;36:327–32, http://dx.doi.org/10.1007/s00261-010-9651-3.
71. Trenker C, Dietrich CF, Ziegler E, Neesse A, Görg C. B-mode ultrasound and contrast-enhanced ultrasound (CEUS) of histological confirmed omental lesions: retrospective analysis of n = 44 patients. Z Gastroenterol. 2019;57:945–51, http://dx.doi.org/10.1055/a-0893-6872.
72. Sidhu PS, Brabrand K, Cantisani V, Correas JM, Cui XW, D'Onofrio M, et al. EFSUMB Guidelines on Interventional Ultrasound (INVUS), Part II. Diagnostic Ultrasound-Guided Interventional Procedures (Long Version). Ultraschall Med. 2015;36:E15–35, http://dx.doi.org/10.1055/s-0035-1554036.
73. Kim JW, Shin SS. Ultrasound-guided percutaneous core needle biopsy of abdominal viscera: tips to ensure safe and effective biopsy. Korean J Radiol. 2017;18:309–22, http://dx.doi.org/10.3348/kjr.2017.18.2.309.
74. Vadvala HV, Furtado VF, Kambadakone A, Frenk NE, Mueller PR, Arellano RS. Image-guided percutaneous omental and mesenteric biopsy: assessment of technical success rate and diagnostic yield. J Vasc Interv Radiol. 2017;28:1569–76, http://dx.doi.org/10.1016/j.jvir.2017.07.001.
75. Minhas K, Roebuck DJ, Barnacle A, De Coppi P, Sebire N, Patel PA. Diagnostic yield and safety of ultrasound-guided bowel mass biopsies in children. Pediatr Radiol. 2019;49:1809–15, http://dx.doi.org/10.1007/s00247-019-04472-8.